CHAPTER 3

Results

Anti-chemoinvasive and ECM degradation enzymes inhibition from Red Jasmine Rice (*Oryza sativa* L.)

3.1 Preparation and quantitative determination of phytochemicals in red rice fractions

3.1.1 Preparation of red rice fractions

The whole grain of red rice was extracted with 70% ethanol. The yield of crude ethanolic extract (CEE) was obtained as 0.61% w/v. The CEE, a starting material was sequentially liquid-liquid partitioned with hexane, dichloromethane, ethyl acetate and water as described in Section 2.2. The water fraction had the highest yield of 56.86%, followed by Hex (18.32%), DCM (3.06%), EtOAc (1.62%) fractions.

3.1.2 The total phenolic contents in the red rice fractions as determined by colorimetric assay

Phenolics, flavonoids, anthocyanin and proanthocyanidins are typically known as phytochemical antioxidants. The total phenolic content (TPC) in the fractions was quantitatively measured by Folin assay as described in Section 2.2. The TPC was expressed in the terms as mg of gallic acid equivalent. As shown in Table 3.1, TPC in the fractions ranged from 29.90±4.33 to 143.91±0.44 mg gallic acid/g extract. The highest quantity of phenolics was found in CEE, followed by water, EtOAc, DCM and Hex fractions, respectively.

3.1.3 The total flavonoid contents in the red rice fractions as determined by colorimetric assay

The quantitative analysis of TFC in the fractions was described in Section 2.2. The TFC was expressed in the terms of mg of catechin equivalent. As shown in Table 3.1, the TFC in the fractions ranged from 91.24±1.52 to 0.15±0.00 mg catechin/g extract. The TFC result was similar to that of the TPC, the highest quantity of flavonoids was in CEE, followed by water, EtOAc, DCM and Hex fractions, respectively.

3.1.4 The total proanthocyanidin contents in the red rice fractions as determined by colorimetric assay

Proanthocyanidins are well known as health-promoting compounds found in medicinal plants, foods and beverages. The vanillin assay in methanol is generally recognized as the best solution for the quantification of proanthocyanidins. In this study, the colorimetric assay of proanthocyanidin in the five fractions was described in Section 2.2. The total proanthocyanidin content was expressed in terms of mg of catechin equivalent. As shown in Table 3.1, the proanthocyanidin content was found highest in CEE, followed by the water fraction, but was not detected in Hex, DCM and EtOAc fractions.

3.1.5 The total anthocyanidin contents in the red rice fractions as determined by colorimetric assay

Anthocyanins are the group of natural antioxidants in fruits and vegetables and have red, violet and blue pigments, giving these produce vivid colors. The pH differential method (AOAC) was described in Section 2.2. The content of total anthocyanin was calculated as cyanidin-3-chloride equivalent. As shown in Table 3.1, a slight amount of anthocyanin in all fractions was detected at a range of 0.012±0.001 to 0.092±0.003 mg cyanidin-3-chloride/g extract.

3.1.6 Quantitative analysis of polyphenols in the red rice fractions by high-performance liquid chromatography (HPLC)

Plant phenolics include phenolics acids, flavonoids, proanthocyanidins and anthocyanins. Liquid–liquid extraction is a method for isolation of phenolic and flavonoid compounds. Phenolic acids are composed of two classes: hydroxybenzoic acid derivatives and hydroxycinnamic acid derivatives. Examples of the first group are gallic acid, protocatechuic acid, vanillic acid and that of the second group are chlorogenic acid, coumaric acid and ferulic acid. In this study, content of phenolic and flavonoid compounds in red rice fractions was determined by HPLC. The chromatographic gradient system was described in Section 2.2. As shown in Table 3.2, all fractions contained protocatechuic, vanillic, chlorogenic, coumaric, ferulic and catechin, but the Hex fraction could not detect only coumaric and ferulic acid. Chlorogenic was the major phenolic acids of CEE and water fractions. Catechin and protocatechuic were predominantly found in EtOAc. On the other hand, catechin was the major bioflavonoid in DCM followed by Hex fractions but less than that in EtOAc fraction.

3.1.7 Quantitative analysis of tocopherol, tocotrienol derivatives in the red rice fractions by high-performance liquid chromatography

Whole grain of rice contains tocopherols, tocotrienols and γ-oryzanol which have health benefits. The δ-, γ-, β-, α-tocopherol and tocotrienol compounds were analyzed by HPLC as described in Section 2.2. The HPLC chromatogram of standards showed the eight main peaks of δ-, γ-, β-, α-tocotrienols and tocopherols at the retention time (RT) values of 14.915, 19.049, 19.817, 24.336, 28.049, 36.617, 38.449 and 48.150 min, respectively. As shown in Table 3.3, γ- tocotrienol was the main component in Hex fraction, followed by DCM and CEE fractions, respectively, but not in EOAc and water fractions. Only the Hex fraction had all four vitamin E analogs containing γ- tocotrienol (2.78±0.02 mg/g extract) followed by α–

tocotrienol (0.04±0.04 mg/g extract), γ-tocopherol (0.20±0.03 mg/g extract) and δ-tocotrienol (0.002±0.002 mg/g extract), respectively, but was not detected in other fractions.

3.1.8 Quantitative analysis of γ-oryzanol in the red rice fractions by high-performance liquid chromatography

Gamma-oryzanol is the major bioactive component in rice. The determination of the γ-oryzanol content in red rice fractions by HPLC was described in Section 2.2. Compared to the standards, the chromatogram of the red rice fractions showed the four main peaks of cycloartenyl ferulate, 24-methylenecycloartanyl ferulate, campesteryl ferulate and sitosteryl ferulate at the retention times (RT) of 32.110, 35.231, 37.654 and 43.427 min, respectively. As shown in Table 3.3, the γ-oryzanol was the major component in all fractions and the Hex fraction contained the highest level, followed by DCM, CEE, water and EtOAc fractions, respectively.

Table 3.1 Phytochemical constituents of the red rice fractions by colormetric method. The data showed average values from 3 time experiments (mean ± SD)

Content (mg/g extract)	**Fractions**				
	CEE	**Hex**	**DCM**	**EtOAc**	**Water**
TPC	143.91±0.44	29.90±4.33	30.78±4.15	100.75±4.35	129.95±2.56
TFC	91.24±1.52	0.15±0.00	0.27±0.47	52.71±1.59	88.94±3.02
TPAC	59.56±5.08	0.010±0.009	0.015±0.007	0.012±0.008	48.70±2.06
TAC	0.020±0.015	0.016±0.009	0.012±0.001	0.092±0.003	0.030±0.001

Table 3.2 Quantitative analysis of polyphenols in the red rice fractions by HPLC. The data showed average values from 3 time experiments (mean ± SD)

Content (mg/g extract)	**Fractions**				
	CEE	**Hex**	**DCM**	**EtOAc**	**Water**
Protocatechuic	0.45±0.011	0.17±0.01	0.64±0.06	56.68±7.85	0.35±0.06
Vanillic	0.14±0.003	0.09±0.01	4.57±0.14	12.18±2.07	0.48±0.18
Chlorogenic	1.18±0.141	0.40±0.09	0.15±0.003	0.91±0.64	1.89±0.19
Coumaric	0.03±0.001	ND	0.11±0.07	7.76±0.63	0.02±0.02
Ferulic	0.12±0.006	ND	1.48±0.18	13.73±2.38	0.06±0.06
Catechin	0.48±0.16	0.49±0.23	21.22±0.36	65.75±4.33	0.51±0.03

ND = not detectable

Table 3.3 Quantitative analysis of tocotrienol, tocopherol and γ-oryzanol in the red rice fractions by HPLC. The data showed average values from 2 time experiments (mean ± SD)

Compounds (mg/g extract)	**Fractions**				
	CEE	**Hex**	**DCM**	**EtOAc**	**Water**
δ-T3	ND	0.002±0.002	ND	ND	ND
γ-T3	1.05±0.42	2.78±0.02	1.97±0.23	ND	ND
α-T3	ND	0.04±0.04	ND	ND	ND
γ-T	ND	0.20±0.03	ND	ND	ND
γ-oryzanol	70.82±1.63	127.55±2.57	94.85±6.49	16.13±0.76	ND

ND = not detectable

3.2 Cytotoxicity of CEE, Hex, DCM, EtOAc and water fractions on MDA-MB-231, HT-1080 human invasive cells

The effect of various concentrations of five red rice fractions (0-100 μg/ml) on MDA-MB-231 and HT-1080 cells viability were determined by MTT method as described in Section 2.4. After treating the cells with various concentrations of five red rice fractions for 48 h., the percent of cells survival was investigated. The percentage of cell viability was calculated for the IC_{20} and IC_{50} value (the concentration at which 80% and 50% of cells survive, respectively). As shown in Figures 3.1-3.5 and Table 3.4-3.8, The IC_{20} and IC_{50} of the fractions were more than 100 μg/ml, suggested that CEE, Hex, DCM, EtOAc and water fractions did not cytotoxic to the cell lines. Based on this data the evaluation of anti-invasion properties of the red rice fractions in human breast cancer and human fibrosarcoma invasive cells could be focused upon.

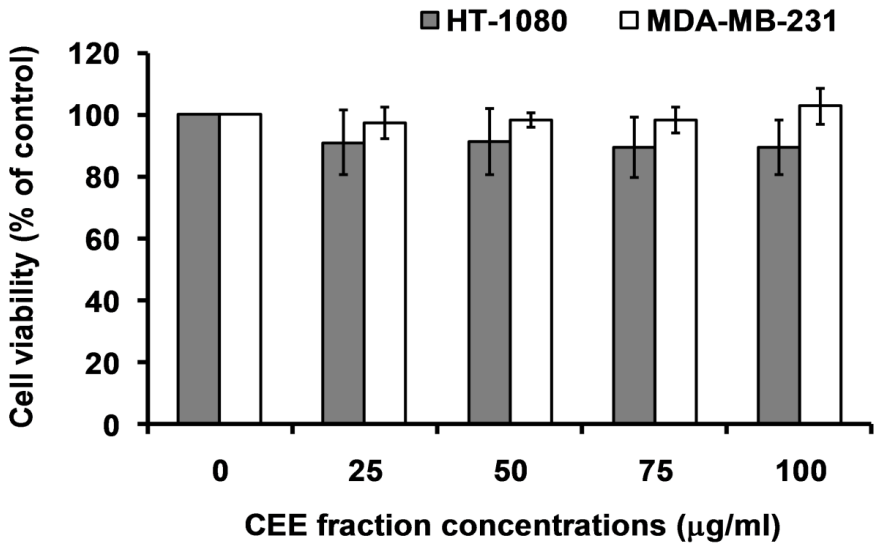

Figure 3.1 Cytotoxicity of CEE fraction on HT-1080 and MDA-MB-231 cells. HT-1080 and MDA-MB-231 cells (1.5×10^3 cell/wells) were treated with 0-100 μg/ml of CEE fraction for 2 days. The cell viability was determined by MTT method. The data showed average values from 3 time experiments (mean ± SD).

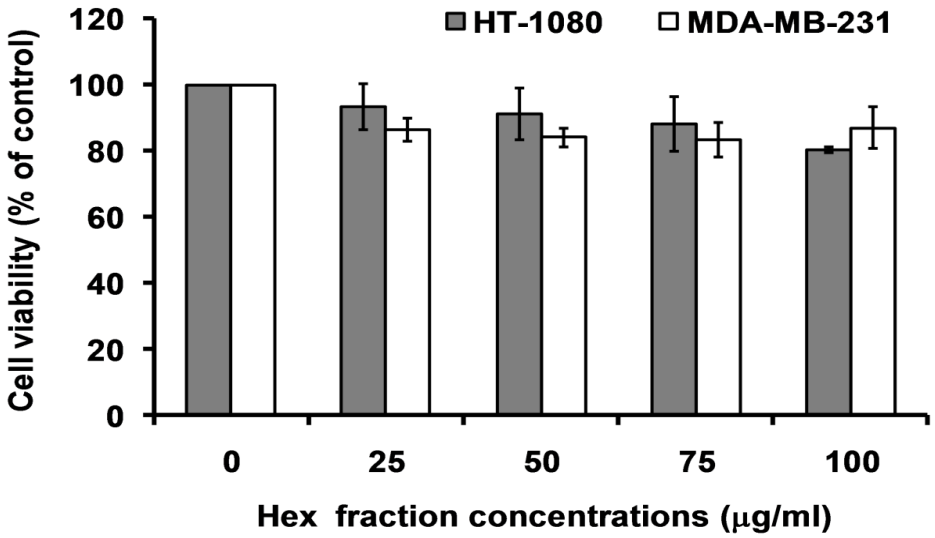

Figure 3.2 Cytotoxicity of Hex fraction on HT-1080 and MDA-MB-231 cells. HT-1080 and MDA-MB-231 cells (1.5×10^3 cell/wells) were treated with 0-100 μg/ml of Hex fraction for 2 days. The cell viability was determined by MTT method. The data showed average values from 3 time experiments (mean ± SD).

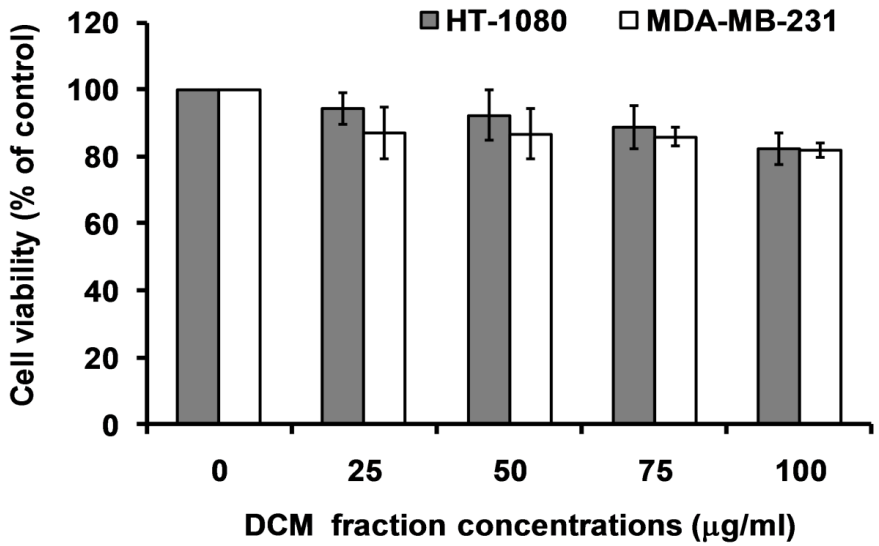

Figure 3.3 Cytotoxicity of DCM fraction on HT-1080 and MDA-MB-231 cells. HT-1080 and MDA-MB-231 cells (1.5×10^3 cell/wells) were treated with 0-100 μg/ml of DCM fraction for 2 days. The cell viability was determined by MTT method. The data showed average values from 3 time experiments (mean ± SD).

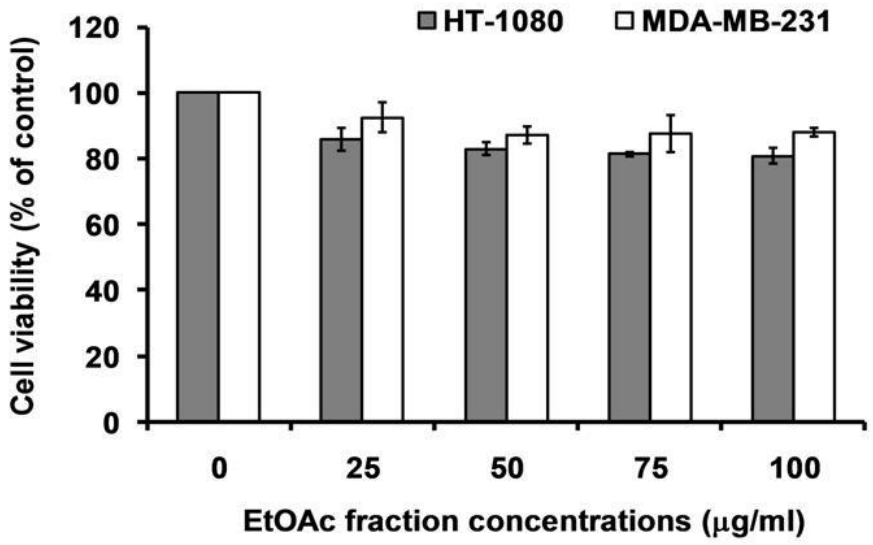

Figure 3.4 Cytotoxicity of EtOAc fraction on HT-1080 and MDA-MB-231 cells. HT-1080 and MDA-MB-231 cells (1.5 x10^3 cell/wells) were treated with 0-100 μg/ml of EtOAc fraction for 2 days. The cell viability was determined by MTT method. The data showed average values from 3 time experiments (mean ± SD).

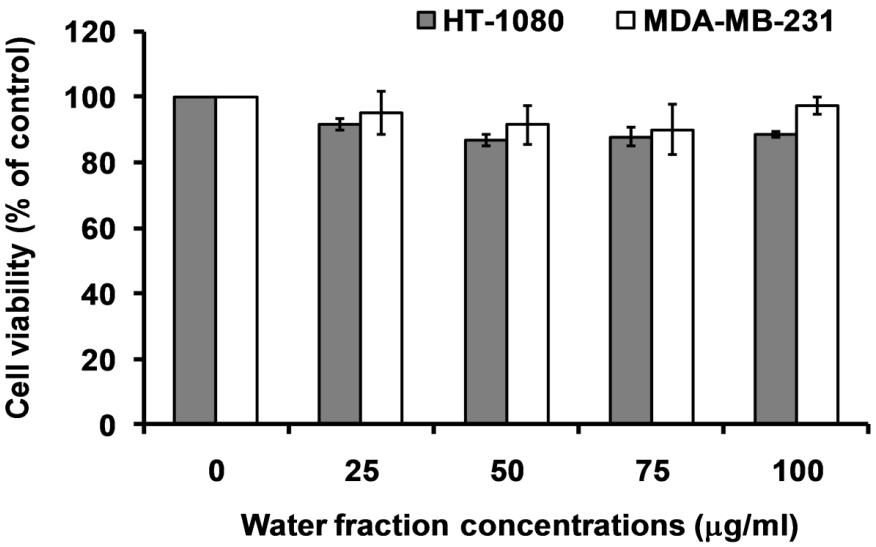

Figure 3.5 Cytotoxicity of water fraction on HT-1080 and MDA-MB-231 cells. HT-1080 and MDA-MB-231 cells (1.5 x10^3 cell/wells) were treated with 0-100 μg/ml of water fraction for 2 days. The cell viability was determined by MTT method. The data showed average values from 3 time experiments (mean ± SD).

Table 3.4 Cytotoxicity of CEE fraction on HT-1080 and MDA-MB-231 cells. The data showed average values from 3 time experiments (mean ± SD)

CEE fraction concentrations (µg/ml)	**Cell viability (% of control)**	
	HT-1080	**MDA-MB-231**
0	100±0.0	100±0.0
25	100±10.4	97±5.3
50	91±10.7	98±2.5
75	91±9.6	98±4.2
100	89±8.9	103±6.0

Table 3.5 Cytotoxicity of Hex fraction on HT-1080 and MDA-MB-231 cells. The data showed average values from 3 time experiments (mean ± SD)

Hex fraction concentrations (µg/ml)	**Cell viability (% of control)**	
	HT-1080	**MDA-MB-231**
0	100±0.0	100±0.0
25	100±6.8	86±3.7
50	93±7.7	84±3.0
75	91±8.2	83±5.25
100	88±0.9	87±6.2

Table 3.6 Cytotoxicity of DCM fraction on HT-1080 and MDA-MB-231 cells. The data showed average values from 3 time experiments (mean ± SD)

DCM fraction concentrations (µg/ml)	**Cell viability (% of control)**	
	HT-1080	**MDA-MB-231**
0	100±0.0	100±0.0
25	94±4.6	89±9.7
50	92±7.4	89±9.1
75	89±6.4	87±1.9
100	82±4.8	82±2.6

Table 3.7 Cytotoxicity of EtOAc fraction on HT-1080 and MDA-MB-231 cells. The data showed average values from 3 time experiments (mean ± SD)

EtOAc fraction concentrations (µg/ml)	**Cell viability (% of control)**	
	HT-1080	**MDA-MB-231**
0	100±0.0	100±0.0
25	86±3.6	94±5.7
50	83±1.8	87±3.7
75	81±0.7	85±5.7
100	81±2.4	88±1.7

Table 3.8 Cytotoxicity of water fraction on HT-1080 and MDA-MB-231 cells. The data showed average values from 3 time experiments (mean ± SD)

Water fraction concentrations (µg/ml)	**Cell viability (% of control)**	
	HT-1080	**MDA-MB-231**
0	100±0.0	100±0.0
25	92±1.7	95±6.7
50	87±1.8	91±6.0
75	88±3.0	90±7.6
100	89±0.7	97±2.5

3.3 Effect of red rice fractions, phenolic acids, grape seed proanthocyanidin, γ-tocotrienol and γ-oryzanol on MDA-MB-231 and HT-1080 cells invasion

3.3.1 Anti-invasive effect of CEE, Hex, DCM, EtOAc and water fractions on MDA-MB-231 and HT-1080 cells

Tumor cell invasion is a key step in the metastasis process whereby cells develop the ability to invade the membrane lipid-bilayer and extracellular matrix. The enzymatic proteolysis of the membrane and extracellular matrix requires several proteases for cell invasion to be a successful. To elucidate whether red rice fractions have anti-invasive property on human cancer cells invasion, Boyden chamber assay was determined as described in Section 2.5. As shown in Figure 3.6-3.7 and Table 3.9, treatment of the cells with 100 μg/ml of CEE, Hex, DCM and water fractions for 16 h significantly decreased MDA-MB-231 cells invasion by 20%, 64%, 66% and 60%, respectively, while decreasing HT-1080 cells invasion by 27%, 41%, 34 % and 35%, respectively. On the other hand, EtOAc fraction had no effect on the cells invasion. In addition, Hex, DCM and water fractions decreased the invasion of MDA-MB-231 cells through the Matrigel in a dose dependent manner when compared to the control, with IC_{50} of 51±2.5, 45±1.88 and 72±1.74 μg/ml, respectively (Figure 3.8-3.10 and Table 3.10).

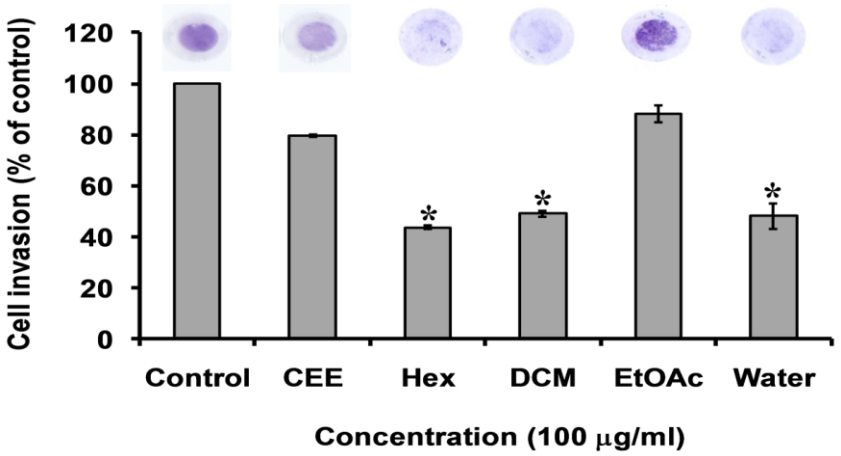

Figure 3.6 Anti-invasive effect of CEE, Hex, DCM, EtOAc and water fractions on MDA-MB-231 cells. The cells ($1x10^5$ cells/well) were seeded in the Matrigel-coated membranes and incubated with or without 100 μg/ml of CEE, Hex, DCM, EtOAc and water fractions. The invaded cells were determined and the data showed average values from 2 time experiments (mean ± SD). (*) $P<0.05$ was considered as statistically significant.

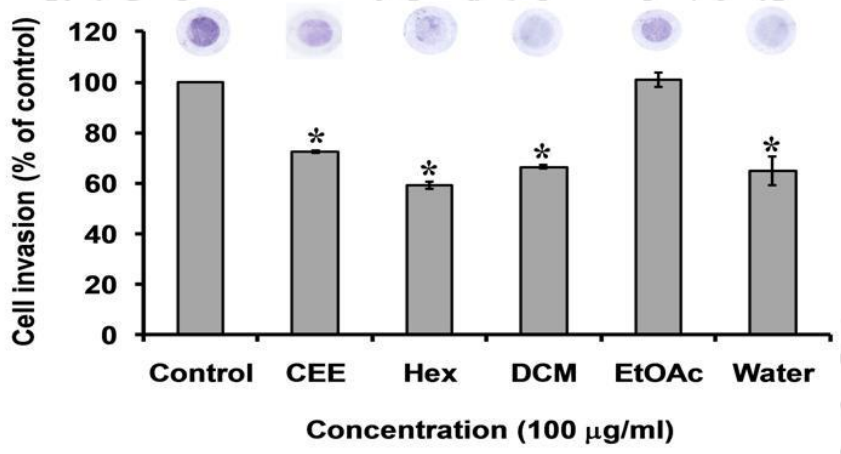

Figure 3.7 Anti-invasive effect of CEE, Hex, DCM, EtOAc and water fractions on HT-1080 cells. The cells ($1x10^5$ cells/well) were seeded in the Matrigel-coated membranes and incubated with or without 100 μg/ml of CEE, Hex, DCM, EtOAc and water fractions. The invaded cells were determined and the data showed average values from 2 time experiments (mean ± SD). (*) $P<0.05$ was considered as statistically significant.

Table 3.9 Anti-invasive effect of CEE, Hex, DCM, EtOAc and water fractions on MDA-MB-231 and HT-1080 cells. The data showed average values from 2 time experiments (mean ± SD)

Red rice fractions concentration (100 µg/ml)	**Cell invasion (% of control)**	
	MDA-MB-231	**HT-1080**
Control	100±0.0	100±0.0
CEE	80±7.39	73±0.3*
Hex	36±12.25*	59±1.6*
DCM	34±8.28*	66±0.7*
EtOAc	100±2.83	101±2.9
Water	40±5.77*	65±5.7*

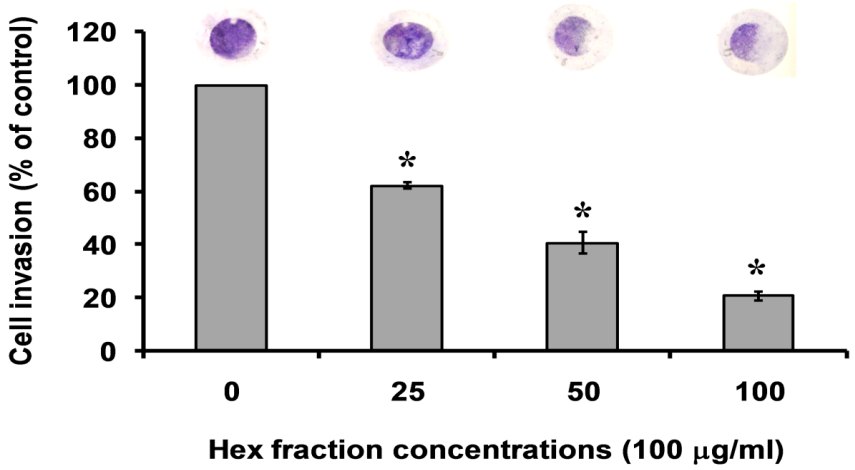

Figure 3.8 Anti-invasive effect of Hex fraction on MDA-MB-231 cells. The cells ($1x10^5$ cells/well) were seeded in the Matrigel-coated membranes and incubated with or without 0-100 μg/ml of Hex fraction. The invaded cells were determined and the data showed average values from 2 time experiments (mean ± SD). (*) $P<0.05$ was considered as statistically significant.

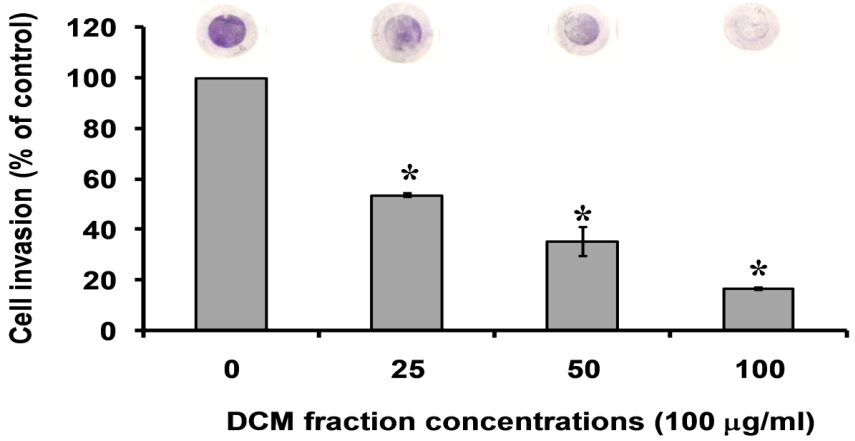

Figure 3.9 Anti-invasive effect of DCM fraction on MDA-MB-231 cells. The cells ($1x10^5$ cells/well) were seeded in the Matrigel-coated membranes and incubated with or without 0-100 μg/ml of DCM fraction. The invaded cells were determined and the data showed average values from 2 time experiments (mean ± SD). (*) $P<0.05$ was considered as statistically significant.

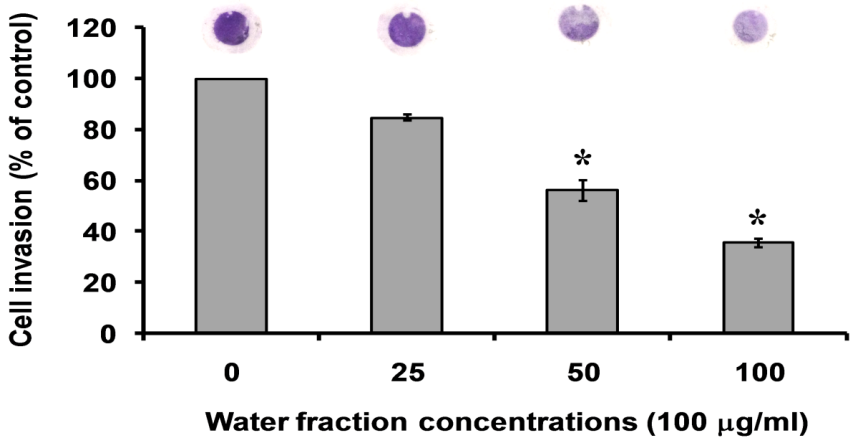

Figure 3.10 Anti-invasive effect of water fraction on MDA-MB-231 cells. The cells ($1x10^5$ cells/well) were seeded in the Matrigel-coated membranes and incubated with or without 0-100 μg/ml of water fraction. The invaded cells were determined and the data showed average values from 2 time experiments (mean ± SD). (*) $P<0.05$ was considered as statistically significant.

Table 3.10 Anti-invasive effect of Hex, DCM and water fraction on MDA-MB-231 cells. The data showed average values from 2 time experiments (mean ± SD)

Concentrations (μg/ml)	**Cell invasion (% of control)**		
	Hex	**DCM**	**Water**
0	100±0.0	100±0.0	100±0.0
25	62±1.2*	54±0.58*	85±3.05
50	41±4.0*	35±5.77*	56±5.77*
100	21±1.7*	17±0.58*	36±1.73*
IC_{50}	51±2.5	45±1.88	72±1.74

3.3.2 Anti-invasive effect of phenolic acid, tocotrienol, γ-oryzanol on MDA-MB-231 cells.

Previous results found that CEE, Hex, DCM and water fractions from red rice significantly decreased MDA-MB-231 and HT-1080 cells invasion. From phytochemicals screening tests, CEE, DCM and water enriched of phenolic acid (protocatechuic acid; Pro, chlorogenic acid; Chl, vanillic acid; Val, ferulic; Fer), flavonoid (catechin; Cat), proanthocyanidin, γ-tocotrienol and γ-oryzanol. On the other hand, Hex fraction mainly contains γ-tocotrienol and γ-oryzanol. Thus, this study elucidated whether these hydrophilic and hydrophobic phytochemicals could effectively inhibit the invasion of MDA-MB-231 cells.

As shown in Figure 3.11A and Table 3.11, treatment of the cells with 50 μg/ml of vanillic acid and ferulic acid for 24 h significantly decreased MDA-MB-231 cells invasion by 35%, and 40%, respectively, while 50 μg/ml of protocatechuic acid and chlorogenic acid slightly decreased MDA-MB-231 cells invasion by 14 % and 18%, respectively. Catechin had no effect on the cells invasion. The estimate concentration of vanillic acid and ferulic acid in our extract (100 μg/ml) was 1 μg/ml. Treatment the cells with this concentration, it then showed only slightly decreasing effect on the cells invasion (Figure 3.11B and Table 3.12.). In addition, the grape seed proanthocyanidin at 1, 5 and 10 μg/ml significantly decreased the cell invasion by 79±3.17%, 71±7.87% and 54±13.95%, respectively (Figure 3.12A and Table 3.13). γ-tocotrienol (10 μg/ml) and γ-oryzanol (50 μg/ml) significantly decreased the invasion of MDA-MB-231 cells as compared to the control by 50±4.4 and 62±10.3%, respectively (Figure 3.12B and Table 3.14).

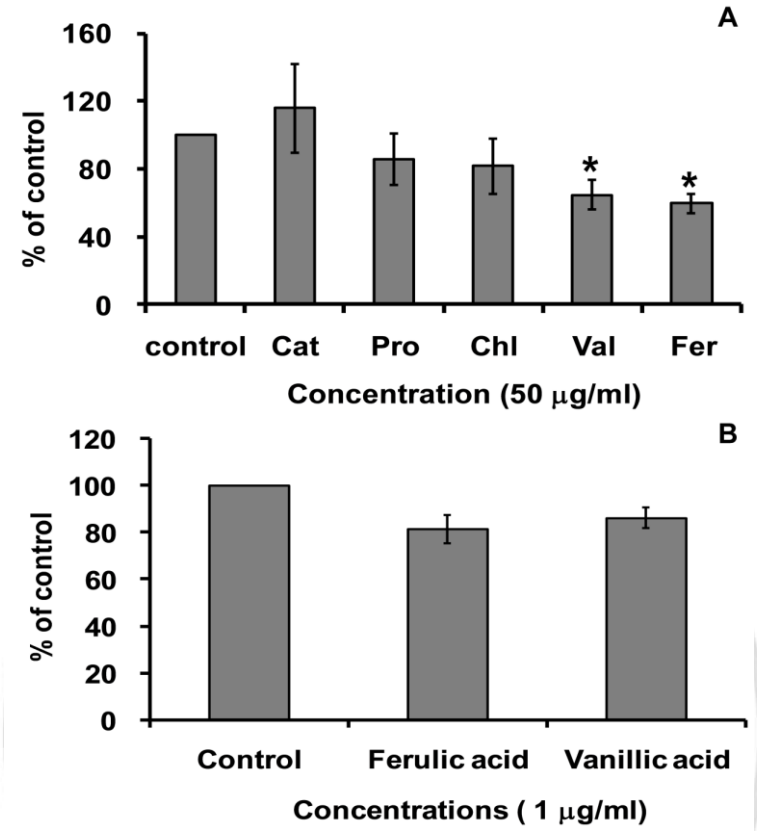

Figure 3.11 Anti-invasive effect of catechin (Cat), protocatechuic acid (Pro), chlorogenic acid (Chl), vanillic acid (Val) and ferulic acid (Fer) on MDA-MB-231 cells. The cells ($1x10^5$ cells/well) were seeded in the Matrigel-coated membranes and incubated with or without the indicated compounds. The invaded cells were determined and the data showed average values from 2 time experiments (mean ± SD). (*) $P<0.05$ was considered as statistically significant.

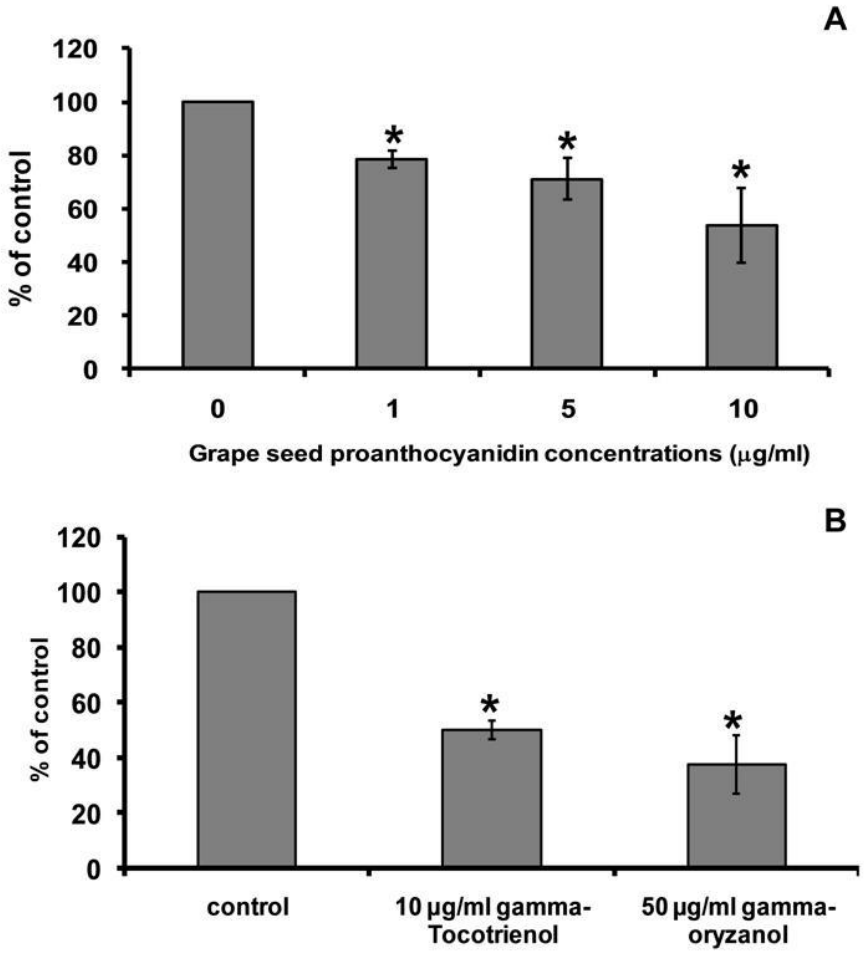

Figure 3.12 Anti-invasive effect of grape seed proanthocyanidin (A), γ-tocotrienol and γ-oryzanol (B) on MDA-MB-231 cells. The cells ($1x10^5$ cells/well) were seeded in the Matrigel-coated membranes and incubated with or without the indicated compounds. The invaded cells were determined and the data showed average values from 2 time experiments (mean ± SD). (*) $P<0.05$ was considered as statistically significant.

Table 3.11 Anti-invasive effect of catechin, protocatechuic acid, chlorogenic acid, vanillic acid and ferulic acid on MDA-MB-231 cells. The data showed average values from 2 time experiments (mean ± SD)

Compounds (50 µg/ml)	**Cell invasion (% of control)**
Control	100±0.0
Catechin	116±26.1
Protocatechuic acid	86±15.0
Chlorogenic acid	82±16.3
Vanillic acid	65±8.8*
Ferulic acid	60±5.7*

Table 3.12 Anti-invasive effect of vanillic acid and ferulic acid (1 µg/ml) on MDA-MB-231 cells. The data showed average values from 2 time experiments (mean ± SD)

Compounds (1 µg/ml)	**Cell invasion (% of control)**
Control	100±0.0
Vanillic acid	81±6.24
Ferulic acid	86±4.51

Table 3.13 Anti-invasive effect of grape seed proanthocyanidin on MDA-MB-231 cells. The data showed average values from 2 time experiments (mean ± SD)

Grape seed proanthocyanidin concentration (µg/ml)	**Cell invasion (% of control)**
0	100±0.00
1	79±3.17*
5	71±7.87*
10	54±13.95*

Table 3.14 Anti-invasive effect of γ-tocotrienol and γ-oryzanol on MDA-MB-231 cells. The data showed average values from 2 time experiments (mean ± SD)

Compounds	**Cell invasion (% of control)**
Control	100±0.00
γ-tocotrienol (10 µg/ml)	50±4.43*
γ-oryzanol (50 µg/ml)	38±10.28*

3.4 Effect of CEE, Hex, DCM, EtOAc and water fractions on secretion of ECM degradation enzymes

3.4.1 Effect of the CEE, Hex, DCM, EtOAc and water fractions on the secretion of MMP-2 and MMP-9 from HT-1080 cells

MMPs are required and facilitated for cancer migration and invasion by the breakdown of the basement membrane and extracellular matrix. Since MMPs are closely related with cancer metastasis they are important for ECM degradation. To clarify, if MMP-2 and MMP-9 were involved in the anti-invasive effect by five red rice fractions, the cells were allowed to treat with 0-100 μg/ml of the fractions for 24 h. The MMP-2 and MMP-9 secretions were analyzed by gelatin zymography as described in Section 2.6 and the intensity of degradation bands was quantified. As shown in Figure 3.13-3.17, the results demonstrated that 100 μg/ml of CEE, Hex, DCM and water fractions could inhibit MMP-2 secretion from HT-1080 by 41%, 70%, 6% and 12%, respectively. Similar concentrations of CEE, Hex, DCM and water fractions inhibited MMP-9 secretion by 46%, 44%, 39% and 26%, respectively. In contrast, EtOAc fraction showed slightly effect on the MMPs secretions from HT-1080 cells. The effects of each fraction are summarized in Table 3.15-3.19.

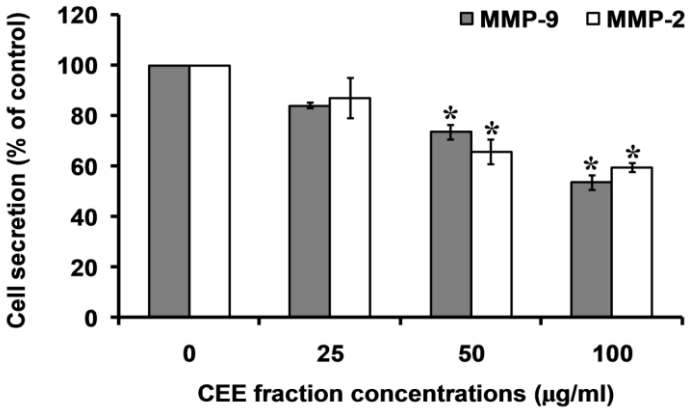

Figure 3.13 Effect of the CEE fraction on MMP-2 and MMP-9 secretions from HT-1080 cells. The HT-1080 cells ($1x10^5$ cells/well) were incubated with 0-100 µg/ml of CEE fraction for 2 days. The MMP-2 and MMP-9 gelatinolytic activities were analyzed by gelatin zymography. The intensity of the bands was evaluated with quantitative densitometry and the data showed average values from 3 time experiments (mean ± SD). (*) $P<0.05$ was considered as statistically significant.

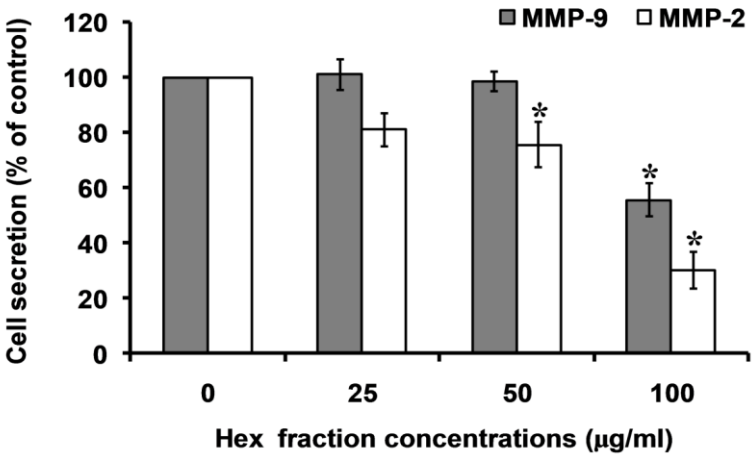

Figure 3.14 Effect of the Hex fraction on MMP-2 and MMP-9 secretions from HT-1080 cells. The HT-1080 cells ($1x10^5$ cells/well) were incubated with 0-100 µg/ml of Hex fraction for 2 days. The MMP-2 and MMP-9 gelatinolytic activities were analyzed by gelatin zymographic assay. The intensity of the bands was evaluated with quantitative densitometry and the data showed average values from 3 time experiments (mean ± SD). (*) $P<0.05$ was considered as statistically significant.

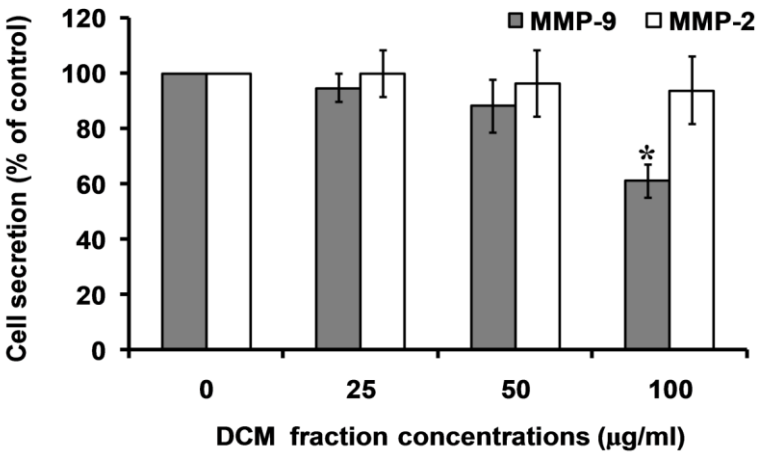

Figure 3.15 Effect of the DCM fraction on MMP-2 and MMP-9 secretions from HT-1080 cells. The HT-1080 cells ($1x10^5$ cells/well) were incubated with 0-100 µg/ml of DCM fraction for 2 days. The MMP-2 and MMP-9 secretions were analyzed by using gelatin zymographic assay. The intensity of the gelatinolytic bands was evaluated with quantitative densitometry and the data showed average values from 3 time experiments (mean ± SD). (*) $P<0.05$ was considered as statistically significant.

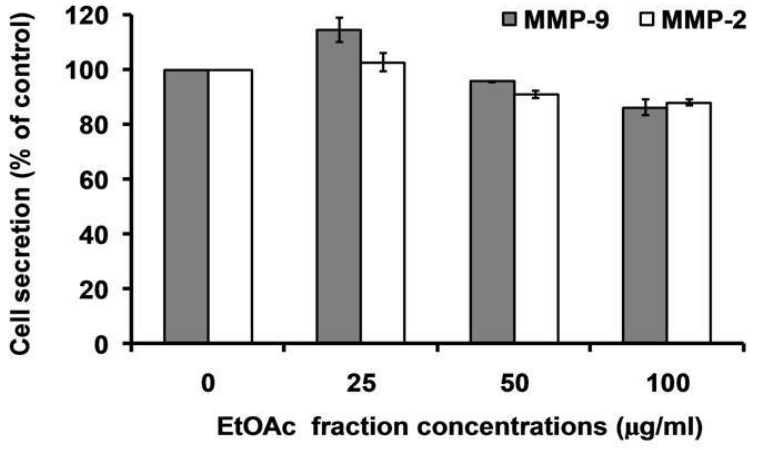

Figure 3.16 Effect of the EtOAc fraction on MMP-2 and MMP-9 secretions from HT-1080 cells. The HT-1080 cells ($1x10^5$ cells/well) were incubated with 0-100 µg/ml of EtOAc fraction for 2 days. The MMP-2 and MMP-9 secretions were analyzed by using gelatin zymographic assay. The intensity of the gelatinolytic bands was evaluated with quantitative densitometry and the data showed average values from 3 time experiments (mean ± SD). (*) $P<0.05$ was considered as statistically significant.

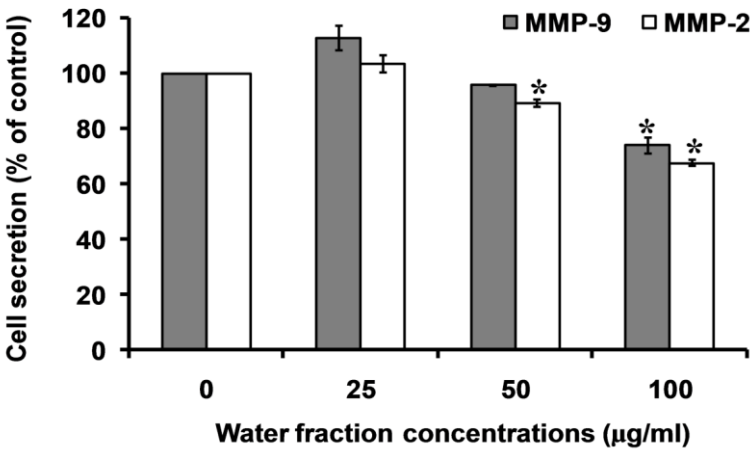

Figure 3.17 Effect of the water fraction on MMP-2 and MMP-9 secretions from HT-1080 cells. The HT-1080 cells ($1x10^5$ cells/well) were incubated with 0-100 µg/ml of water fraction for 2 days. The MMP-2 and MMP-9 secretions were analyzed by using gelatin zymographic assay. The intensity of the gelatinolytic bands was evaluated with quantitative densitometry and the data showed average values from 3 time experiments (mean ± SD). (*) $P<0.05$ was considered as statistically significant.

Table 3.15 Effect of the CEE fraction on MMP-2 and MMP-9 secretions from HT-1080 cells. The data showed average values from 3 time experiments (mean ± SD)

Concentrations (µg/ml)	**MMPs secretion (% of control)**	
	MMP-2	**MMP-9**
0	100±0.0	100±0.0
25	87±8.04	84±1.08
50	66±5.02*	74±2.89*
100	59±1.61*	54±2.89*

Table 3.16 Effect of the Hex fraction on MMP-2 and MMP-9 secretions from HT-1080 cells. The data showed average values from 3 time experiments (mean ± SD)

Concentrations (µg/ml)	**MMPs secretion (% of control)**	
	MMP-2	**MMP-9**
0	100±0.0	100±0.0
25	81±6.0	101±5.6
50	76±8.3*	99±3.5
100	30±6.7*	56±5.9*

Table 3.17 Effect of the DCM fraction on MMP-2 and MMP-9 secretions from HT-1080 cells. The data showed average values from 3 time experiments (mean ± SD)

Concentrations (µg/ml)	**MMPs secretion (% of control)**	
	MMP-2	**MMP-9**
0	100±0.0	100±0.0
25	100±8.5	94.6±5.1
50	96±12.0	88.1±9.7
100	94±12.3	61.0±6.1*

Table 3.18 Effect of the EtOAc fraction on MMP-2 and MMP-9 secretions from HT-1080 cells. The data showed average values from 3 time experiments (mean ± SD)

Concentrations (µg/ml)	**MMPs secretion (% of control)**	
	MMP-2	**MMP-9**
0	100±0.0	100±0.0
25	103±3.1	114±4.5
50	91±1.2	96±0.3
100	88±1.2	86±2.9

Table 3.19 Effect of the water fraction on MMP-2 and MMP-9 secretions from HT-1080 cells. The data showed average values from 3 time experiments (mean ± SD)

Concentrations (µg/ml)	**MMPs secretion (% of control)**	
	MMP-2	**MMP-9**
0	100±0.0	100±0.0
25	103±0.2	113±2.1
50	89±2.6*	96±1.3
100	68±5.9*	74±2.6*

3.4.2 Effect of the CEE, Hex, DCM, EtOAc and water fractions on the secretion of MMP-9 from MDA-MB-231 cells

The combined activity of ECM degradating enzymes increases ECM degradation and potentially increases the tumor cells invasion and metastasis. Thus, decreasing the secretion of ECM degradation enzymes or inhibiting the enzymes activity may lead to furture therapeutic approaches. To determine whether red rice fractions have an inhibitory effect on MMP-9 secretion from MDA-MB-231 cells, the cells were allowed to treat with the fractions at 0, 50, 100 µg/ml for 24 h. Cell supernatants were subjected to gelatin zymographic assay to analyze the secretion of MMP-9. The result demonstrated that MMP-9 secretion from the cells was markedly reduced by HEX fraction in a dose dependent manner with IC_{50} value of 57±3.8 µg/ml (Figure 3.19, Table 3.20). Additional, the reduction of MMP-9 secretion was found in CEE, DCM and water fractions treated cells with IC_{50} values of 95±8.7, 91±3.3 and 95±4.1 µg/ml, respectively, whereas EtOAc fraction had no effect on cell secretion. The inhibitory effect of each fraction is summarized in Figure 3.18-3.22 and Table 3.20.

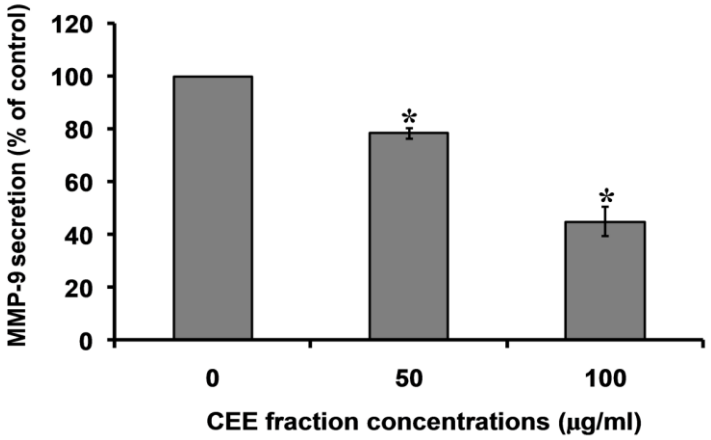

Figure 3.18 Effect of the CEE fraction on MMP-9 secretion from MDA-MB-231 cells. Cells suspension ($1x10^5$ cells/well) was incubated with 0-100 µg/ml of CEE fraction for 2 days. The MMP-9 gelatinolytic activity was analyzed by using gelatin zymographic assay. The intensity of the bands were evaluated with quantitative densitometry and the data showed average values from 3 time experiments (mean ± SD). (*) $P<0.05$ was considered as statistically significant.

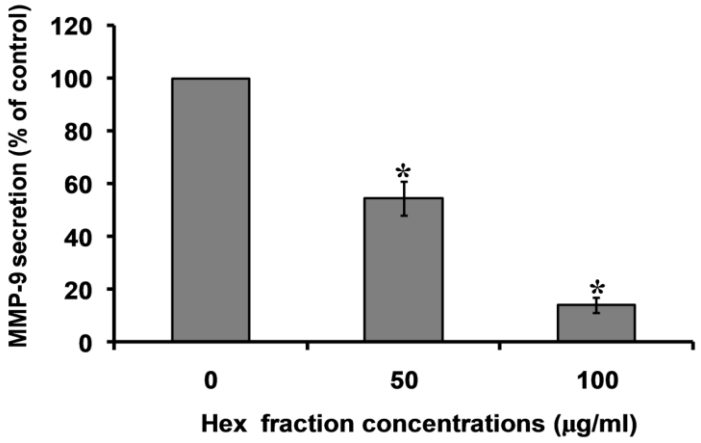

Figure 3.19 Effect of the Hex fraction on MMP-9 secretion from MDA-MB-231 cells. The cells ($1x10^5$ cells/well) were incubated with 0-100 µg/ml of Hex fraction for 2 days. The MMP-9 secretion was analyzed by using gelatin zymographic assay. The intensity of the gelatinolytic bands was evaluated with quantitative densitometry and the data showed average values from 3 time experiments (mean ± SD). (*) $P<0.05$ was considered as statistically significant.

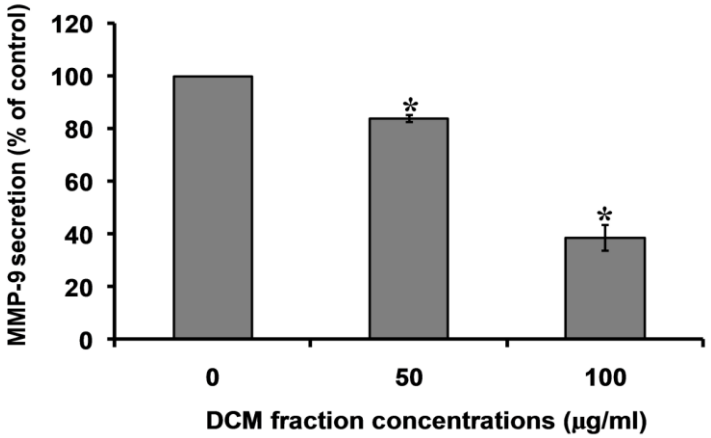

Figure 3.20 Effect of the DCM fraction on MMP-9 secretion from MDA-MB-231 cells. The cells ($1x10^5$ cells/well) were incubated with 0-100 µg/ml of DCM fraction for 2 days. The MMP-9 secretion was analyzed by using gelatin zymographic assay. The intensity of the gelatinolytic bands was evaluated with quantitative densitometry and the data showed average values from 3 time experiments (mean ± SD). (*) $P<0.05$ was considered as statistically significant.

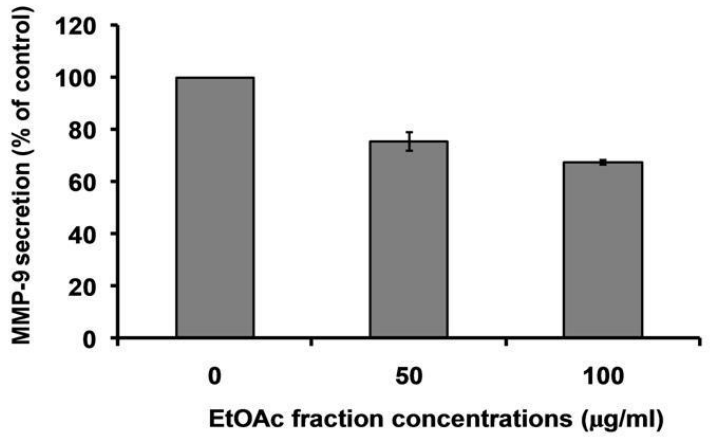

Figure 3.21 Effect of the EtOAc fraction on MMP-9 secretion from MDA-MB-231 cells. The cells ($1x10^5$ cells/well) were incubated with 0-100 µg/ml of EtOAc fraction for 2 days. The MMP-9 secretion was analyzed by using gelatin zymographic assay. The intensity of the gelatinolytic bands was evaluated with quantitative densitometry and the data showed average values from 3 time experiments (mean ± SD). (*) $P<0.05$ was considered as statistically significant.

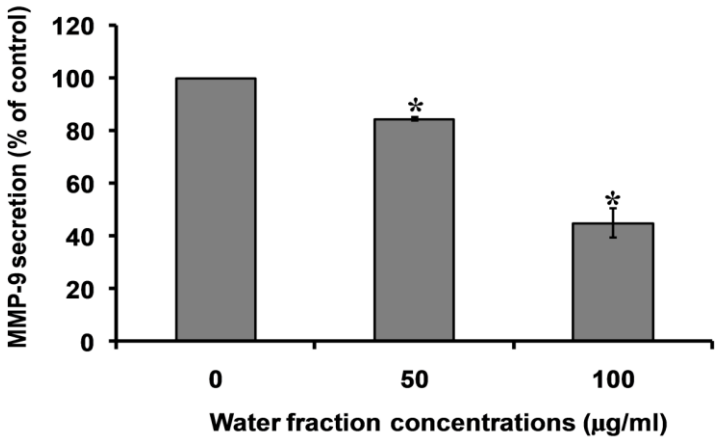

Figure 3.22 Effect of the water fraction on MMP-9 secretion from MDA-MB-231 cells. The cells ($1x10^5$ cells/well) were incubated with 0-100 µg/ml of water fraction for 2 days. The MMP-9 secretion was analyzed by using gelatin zymographic assay. The intensity of the gelatinolytic bands was evaluated with quantitative densitometry and the data showed average values from 3 time experiments (mean ± SD). (*) $P<0.05$ was considered as statistically significant.

Table 3.20 Effect of the CEE, Hex, DCM, EtOAc and water fractions on MMP-9 secretion from MDA-MB-231 cells. The data showed average values from 3 time experiments (mean ± SD)

Concentrations (µg/ml)	**MMP-9 secretion (% of control)**				
	CEE	**Hex**	**DCM**	**EtOAc**	**Water**
0	100±0.0	100±0.0	100±0.0	100±0.0	100±0.0
50	79±2.1*	55±6.4*	84±1.4*	75.5±3.5	85±0.7*
100	45±5.7*	14±2.8*	39±4.9*	67.5±0.7	45±5.7*
IC_{50}	95±8.7	57±3.8	91±3.3	>100	95±4.1

3.5 Effect of CEE, Hex, DCM, EtOAc and water fractions on the activities of enzymes involved in ECM degradation

3.5.1 Effect of the CEE, Hex, DCM, EtOAc and water fractions on MMP-2 and MMP-9 activities of HT-1080 cells

Matrix metalloproteinases like MMP-2 and MMP-9 are the important enzymes in the cancer cell invasion process. Concentrated serum-free medium showed the 72 and 92 kDa digested bands, representing to MMP-2 and MMP-9, respectively. To determine whether red rice fractions have an inhibitory effect on MMP-2 and MMP-9 activities secreted from HT-1080. After loading the medium containing MMP-2 and MMP-9 on preparative gelatin containing polyacrylamide gels, they were subjected to electrophoresis and then allowed to incubate with 0-100 μg/ml of red rice fractions for 24 h. Then, the genolytic bands were scanned by densitometer to estimate the MMP-2 and MMP-9 gelatinolytic activities. As shown in Figure 3.23-3.27 and Table 3.21-3.25, the result demonstrated that MMP-2 and MMP-9 activities were markedly reduced by CEE and water fractions in a dose dependent manner. At 100 μg/ml of Hex fraction significantly reduced only the MMP-9 activity, while the activity of MMP-2 was slightly inhibited. In contrast, the DCM and EtOAc fractions slightly inhibited both MMPs activities.

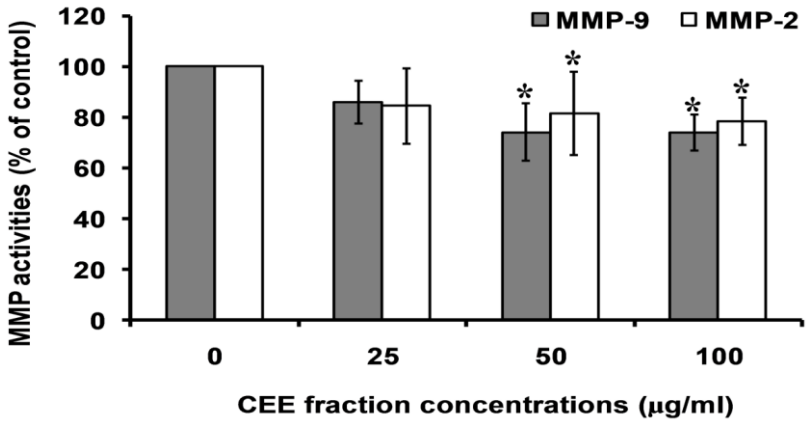

Figure 3.23 Effect of the CEE fraction on MMP-2 and MMP-9 activities of HT-1080 cells. Culture supernatant of HT-1080 was collected and subjected to electrophoresis. The gelatin containing polyacrylamide gels were washed and incubated with 0-100 µg/ml CEE fraction for 24 h. Gelatinolytic acitivity showed as clear band on a blue background. The data showed average values from 3 time experiments (mean ± SD). (*) P<0.05 vs 0 µg/ml

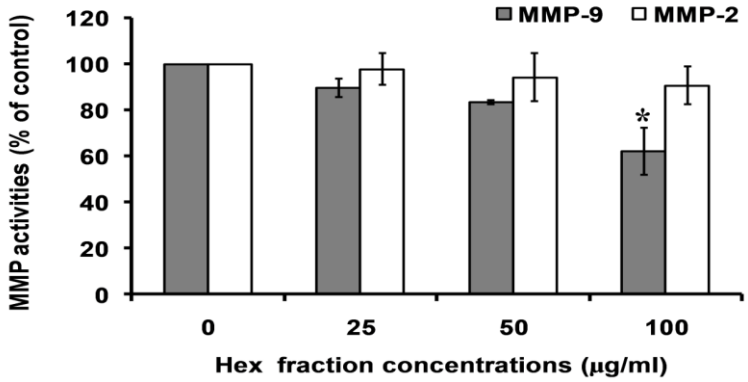

Figure 3.24 Effect of the Hex fraction on MMP-2 and MMP-9 activities of HT-1080 cells. Culture supernatant of HT-1080 was collected and subjected to electrophoresis. The gelatin containing polyacrylamide gels were washed and incubated with 0-100 µg/ml Hex fraction for 24 h. Gelatinolytic acitivity showed as clear band on a blue background. The data showed average values from 3 time experiments (mean ± SD). (*) P<0.05 vs 0 µg/ml

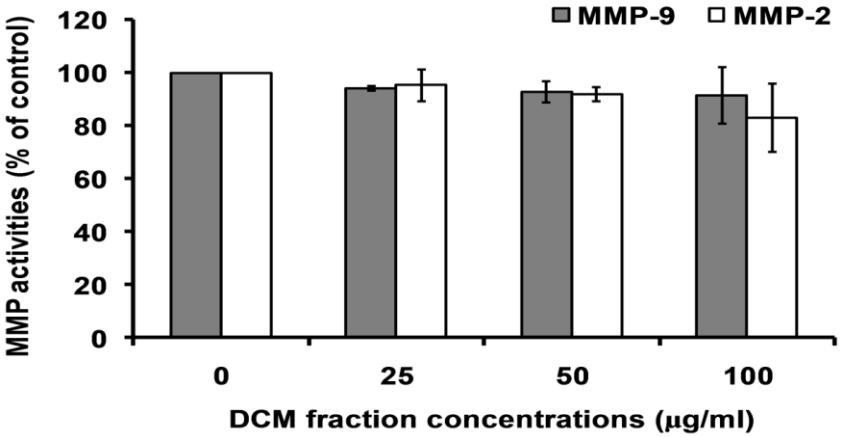

Figure 3.25 Effect of the DCM fraction on MMP-2 and MMP-9 activities of HT-1080 cells. Culture supernatant of HT-1080 was collected and subjected to electrophoresis. The gelatin containing polyacrylamide gels were washed and incubated with 0-100 µg/ml DCM fraction for 24 h. Gelatinolytic acitivity showed as clear band on a blue background. The data showed average values from 3 time experiments (mean ± SD). (*) $P<0.05$ vs 0 µg/ml

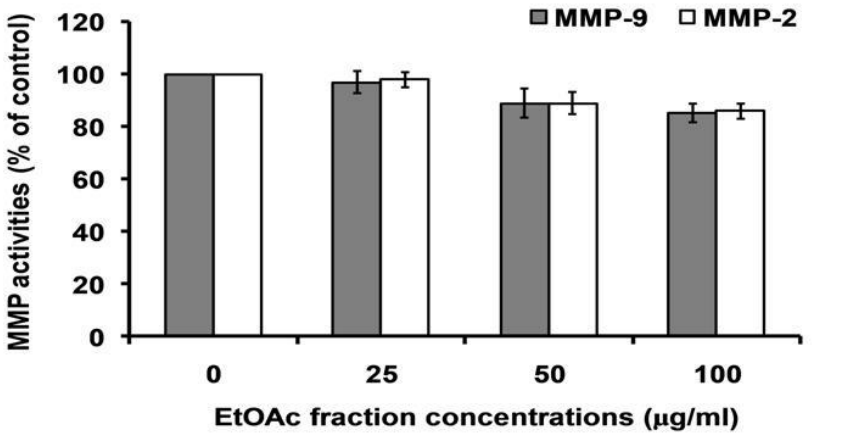

Figure 3.26 Effect of the EtOAc fraction on MMP-2 and MMP-9 activities of HT-1080 cells. Culture supernatant of HT-1080 was collected and subjected to electrophoresis. The gelatin containing polyacrylamide gels were washed and incubated with 0-100 µg/ml EtOAc fraction for 24 h. Gelatinolytic acitivity showed as clear band on a blue background. The data showed average values from 3 time experiments (mean ± SD). (*) $P<0.05$ vs 0 µg/ml

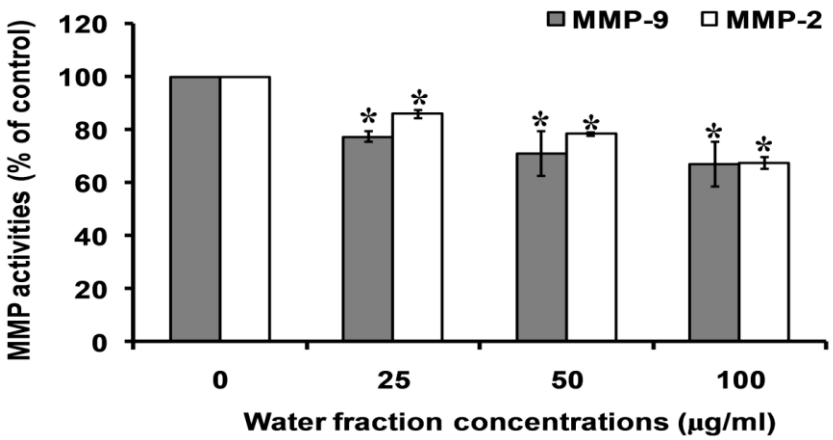

Figure 3.27 Effect of the water fraction on MMP-2 and MMP-9 activities of HT-1080 cells. Culture supernatant of HT-1080 was collected and subjected to electrophoresis. The gelatin containing polyacrylamide gels were washed and incubated with 0-100 μg/ml water fraction for 24 h. Gelatinolytic acitivity showed as clear band on a blue background. The data showed average values from 3 time experiments (mean ± SD). (*) $P<0.05$ vs 0 μg/ml

Table 3.21 Effect of the CEE fraction on MMP-2 and MMP-9 activities from HT-1080 cells. The data showed average values from 3 time experiments (mean ± SD)

Concentrations (µg/ml)	**MMPs activities (% of control)**	
	MMP-2	**MMP-9**
0	100±0.0	100±0.0
25	85±14.85	86±8.49
50	82±16.26*	74±11.31*
100	79±9.19*	74±7.07*

Table 3.22 Effect of the Hex fraction on MMP-2 and MMP-9 activities from HT-1080 cells. The data showed average values from 3 time experiments (mean ± SD)

Concentrations (µg/ml)	**MMPs activities (% of control)**	
	MMP-2	**MMP-9**
0	100±0.0	100±0.0
25	98±6.85	90±3.89
50	94±10.48	83±0.84
100	91±8.18	62±10.23*

Table 3.23 Effect of the DCM fraction on MMP-2 and MMP-9 activities from HT-1080 cells. The data showed average values from 3 time experiments (mean ± SD)

Concentrations (µg/ml)	**MMPs activities (% of control)**	
	MMP-2	**MMP-9**
0	100±0.0	100±0.0
25	95±6.12	94±1.00
50	92±2.83	93±4.14
100	83±13.00	91±10.61

Table 3.24 Effect of the EtOAc fraction on MMP-2 and MMP-9 activities from HT-1080 cells. The data showed average values from 3 time experiments (mean ± SD)

Concentrations (µg/ml)	**MMPs activities (% of control)**	
	MMP-2	**MMP-9**
0	100±0.0	100±0.0
25	98±2.83	97±4.24
50	89±4.24	89±5.66
100	86±2.83	86±3.54

Table 3.25 Effect of the water fraction on MMP-2 and MMP-9 activities from HT-1080 cells. The data showed average values from 3 time experiments (mean ± SD)

Concentrations (µg/ml)	**MMPs activities (% of control)**	
	MMP-2	**MMP-9**
0	100±0.0	100±0.0
25	86±1.41*	78±2.12*
50	79±0.71*	71±8.49*
100	68±2.12*	67±8.49*

3.5.2 Effect of CEE, Hex, DCM, EtOAc and water fractions on the MMP-9 activity secreted from MDA-MB-231 cell.

Matrix metalloproteinases are the important proteolytic enzymes in the invasive process of cancer cell. Concentrated serum-free medium of MDA-MB-231 cells showed the MMP-9 digested bands at 92 kDa. To determine whether red rice fractions have an inhibitory effect on MMP-9 activity of MDA-MB-231 cells. The medium containing MMP-9 was loaded on preparative gelatin containing polyacrylamide gels and subjected to electrophoresis. And then incubation with 0-100 µg/ml of red rice fractions for 24 h, the intensity of genolytic bands was scanned by densitometer to evaluate the activity of MMP-9. As shown in Figure 3.28-3.32 and Table 3.26, the results demonstrated that MMP-9 activity was significantly reduced by CEE, HEX, DCM and water fractions in a concentration dependent manner with IC_{50} values of 55±13.5, 64±8.0, 89±2.0 and 66±10.4 µg/ml, respectively. While EtOAc at concentration of 25, 50 and 100 µg/ml slightly inhibited MMP-9 activity by 15, 13 and 20%, respectively.

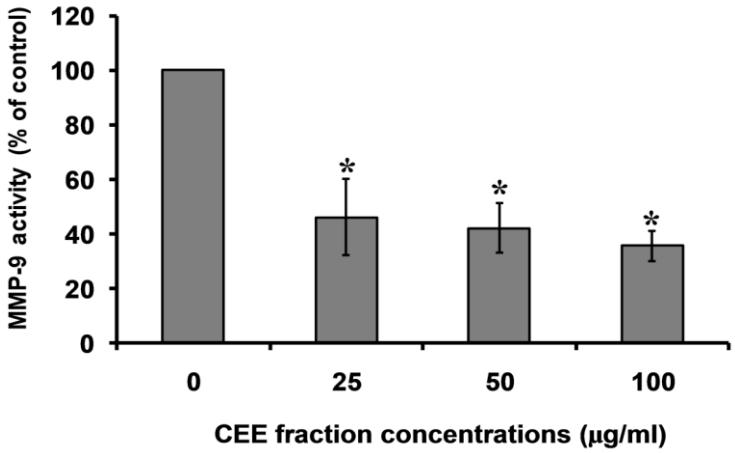

Figure 3.28 Effect of CEE fraction on MMP-9 activity of MDA-MB-231 cell. Culture supernatant of MDA-MB-231 was collected and subjected to electrophoresis. The gelatin containing polyacrylamide gels were washed and incubated with various concentrations of 0-100 µg/ml CEE fraction for 24 h. Gelatinolytic acitivity showed as clear band on a blue background. The data showed average values from 3 time experiments (mean ± SD). (*) P<0.05 vs 0 µg/ml

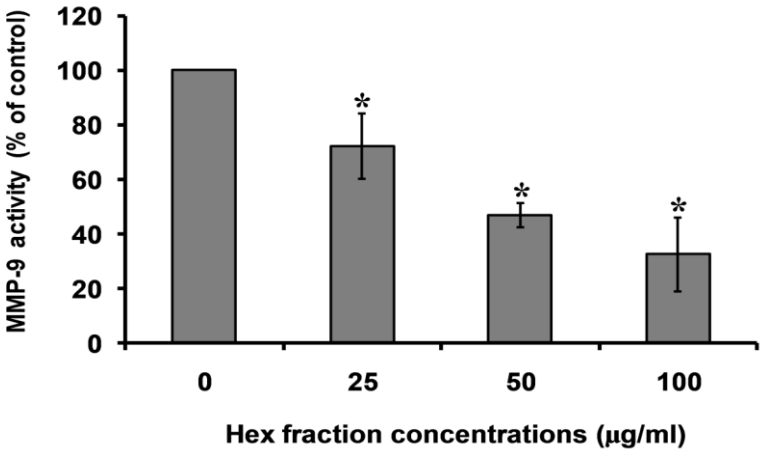

Figure 3.29 Effect of Hex fraction on MMP-9 activity of MDA-MB-231 cell. Culture supernatant of MDA-MB-231 was collected and subjected to electrophoresis. The gelatin containing polyacrylamide gels were washed and incubated with various concentrations of 0-100 µg/ml Hex fraction for 24 h. Gelatinolytic acitivity showed as clear band on a blue background. The data showed average values from 3 time experiments (mean ± SD). (*) P<0.05 vs 0 µg/ml

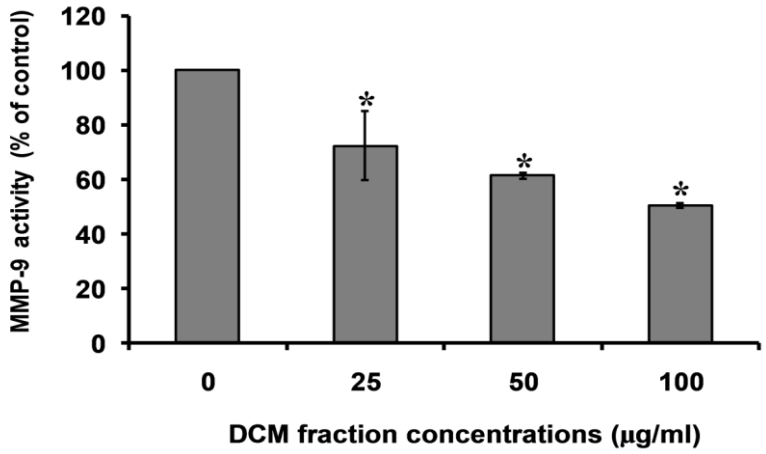

Figure 3.30 Effect of DCM fraction on MMP-9 of MDA-MB-231 cell. Culture supernatant of MDA-MB-231 was collected and subjected to electrophoresis. The gelatin containing polyacrylamide gels were washed and incubated with various concentrations of 0-100 µg/ml DCM fraction for 24 h. Gelatinolytic acitivity showed as clear band on a blue background. The data showed average values from 3 time experiments (mean ± SD). (*) P<0.05 vs 0 µg/ml

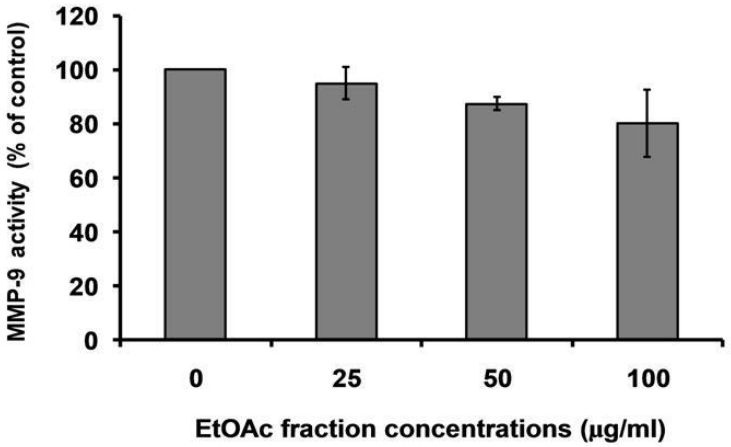

Figure 3.31 Effect of EtOAc fraction on MMP-9 activity of MDA-MB-231 cell. Culture supernatant of MDA-MB-231 was collected and subjected to electrophoresis. The gelatin containing polyacrylamide gels were washed and incubated with various concentrations of 0-100 µg/ml EtOAc fraction for 24 h. Gelatinolytic acitivity showed as clear band on a blue background. The data showed average values from 3 time experiments (mean ± SD). (*) P<0.05 vs 0 µg/ml

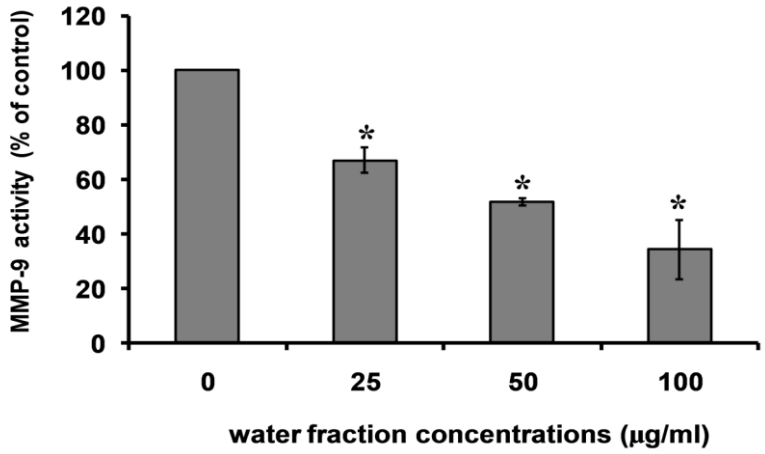

Figure 3.32 Effect of water fraction on MMP-9 activity of MDA-MB-231 cell. Culture supernatant of MDA-MB-231 was collected and subjected to electrophoresis. The gelatin containing polyacrylamide gels were washed and incubated with various concentrations of 0-100 µg/ml water fraction for 24 h. Gelatinolytic acitivity showed as clear band on a blue background. The data showed average values from 3 time experiments (mean ± SD). Statistical analyses were performed using one-way ANOVA. (*) $P<0.05$ vs 0 µg/ml

Table 3.26 Effect of CEE, Hex, DCM, EtOAc and water fractions on MMP-9 activities from MDA-MB-231 cells. The data showed average valuestime e from 3 xperiments (mean ± SD)

Concentrations (µg/ml)	**MMP-9 activity (% of control)**				
	CEE	**Hex**	**DCM**	**EtOAc**	**Water**
0	100±0.0	100±0.0	100±0.0	100±0.0	100±0.0
25	46±13.9*	72±11.9*	72±12.8*	95±5.9	67±4.6*
50	42±9.0*	47±4.5*	61±1.1*	87±2.5	52±1.4*
100	36±5.6*	33±13.4*	50±1.1*	80±12.5	34±11.0*
IC_{50}	55±13.5	64±8.0	89±2.0	>100	66±10.4

3.5.3 Effect of CEE, Hex, DCM, EtOAc and water fractions on collagenase type IV activity

The inhibitory effect of CEE, Hex, DCM, EtOAc and water fractions from red rice extracts on collagenase activities was investigated. The various concentrations (0-100 μg/ml) of the red rice fractions were incubated with DQ gelatin fluorescent substrate. The proteolytic activities of collagenase type IV from *Clostridium histolyticum* (Invitrogen, Merelbeke, Belgium) was measured using a fluorometric assay as described in section 2.10. As shown in Figure 3.33-3.37 and Table 3.27, CEE, HEX, DCM and water fractions significantly inhibited collagenase activity in a concentration-dependent manner with IC_{50} values of 27±0.5, 65±0.5, >200 and 31±0.5 μg/ml, respectively. In contrast, EtOAc fraction had no effect on the activity of collagenase type IV.

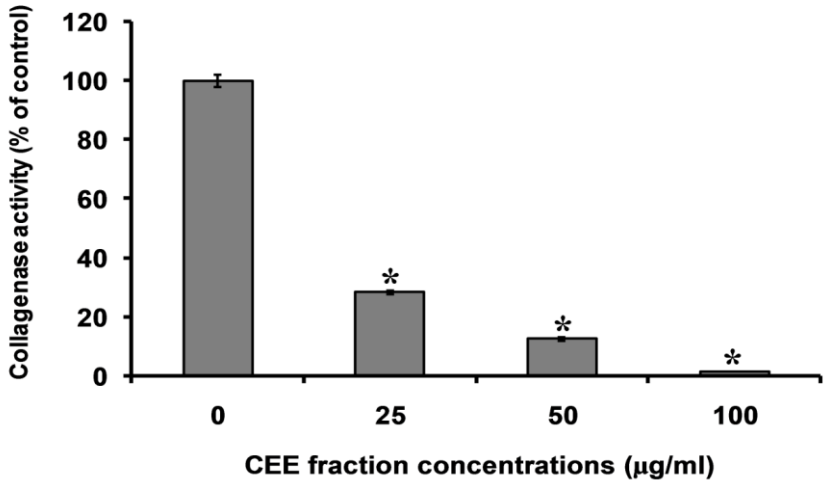

Figure 3.33 Effect of CEE fraction on collagenase type IV activity determined by fluorometric assay. The collagenase with DQ-gelatin fluorescence substrate was incubated with or without the fraction for 30 min. The fluorescent insensity represent collagenase activity. The data showed average values from 3 time experiments (mean ± SD). (*) $P<0.05$ was considered as statistically significant.

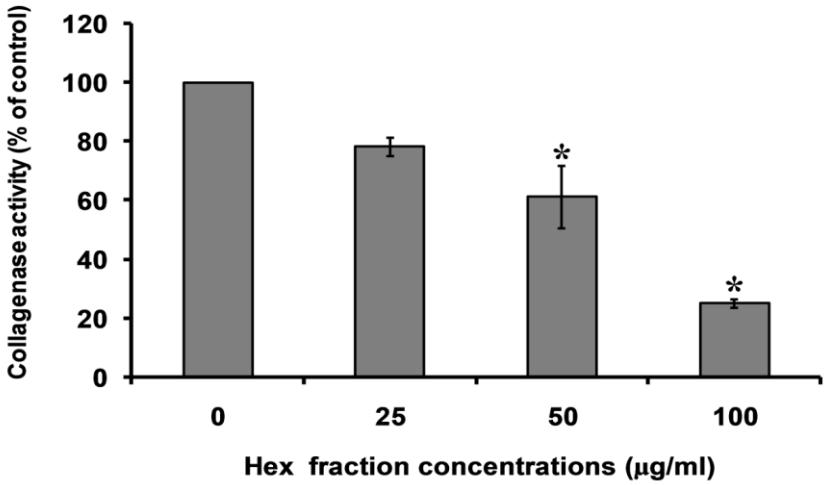

Figure 3.34 Effect of Hex fraction on collagenase type IV activity determine by fluorometric assay. The collagenase with DQ-gelatin fluorescence substrate was incubated with or without the fraction for 30 min. The fluorescent insensity represent collagenase activity. The data showed average values from 3 time experiments (mean ± SD). (*) $P<0.05$ was considered as statistically significant.

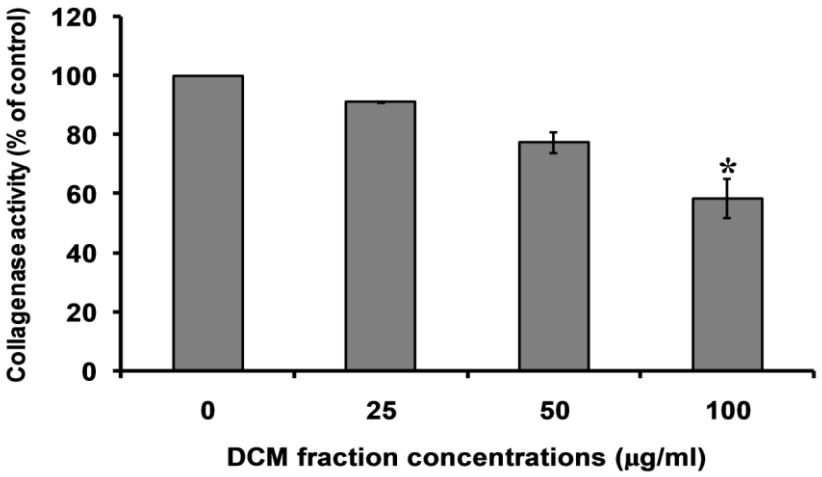

Figure 3.35 Effect of DCM fraction on collagenase type IV activity determine by fluorometric assay. The collagenase with DQ-gelatin fluorescence substrate was incubated with or without the fraction for 30 min. The fluorescent insensity represent collagenase activity. The data showed average values from 3 time experiments (mean ± SD). (*) $P<0.05$ was considered as statistically significant.

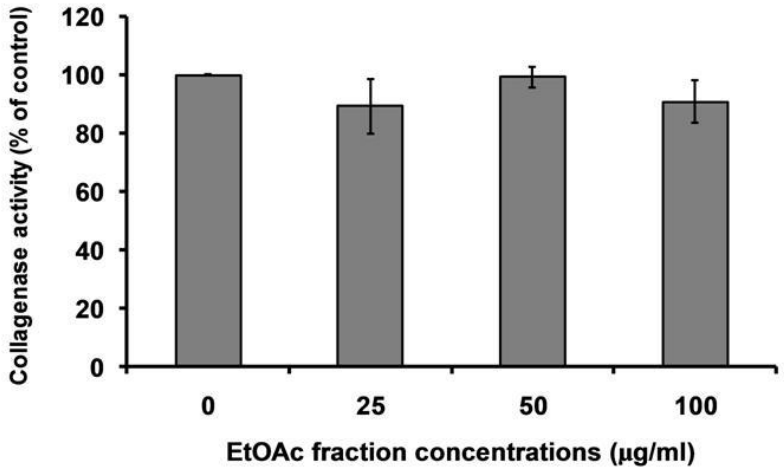

Figure 3.36 Effect of EtOAc fraction on collagenase type IV activity determine by fluorometric assay. The collagenase with DQ-gelatin fluorescence substrate was incubated with or without the fraction for 30 min. The fluorescent insensity represent collagenase activity. The data showed average values from 3 time experiments (mean ± SD). (*) $P<0.05$ was considered as statistically significant.

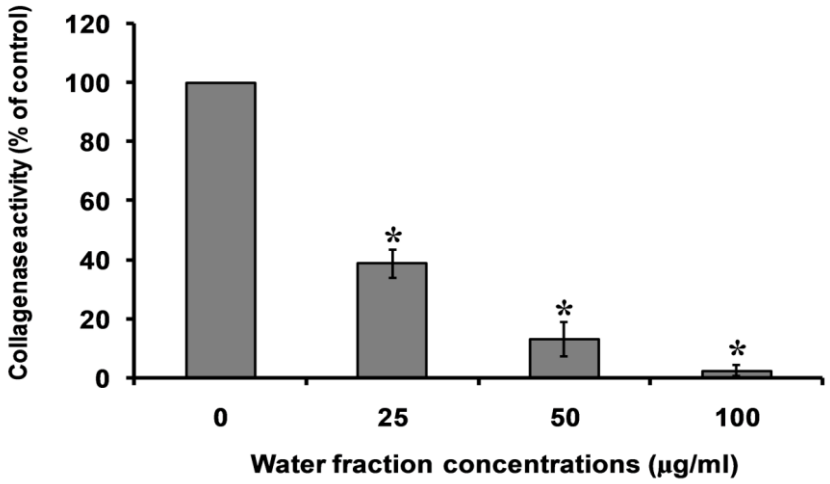

Figure 3.37 Effect of water fraction on collagenase type IV activity determine by fluorometric assay. The collagenase with DQ-gelatin fluorescence substrate was incubated with or without the fraction for 30 min. The fluorescent insensity represent collagenase activity. The data showed average values from 3 time experiments (mean ± SD). (*) $P<0.05$ was considered as statistically significant.

Table 3.27 Effect of CEE, Hex, DCM, EtOAc and water fractions on collagenase type IV activity. The data showed average values from 3 time experiments (mean ± SD)

Concentrations (µg/ml)	**Collagenase type IV activity (% of control)**				
	CEE	**Hex**	**DCM**	**EtOAc**	**Water**
0	100±0.0	100±0.0	100±0.0	100±0.0	100±0.0
25	28±2.0*	78±3.2	91±0.3	89±9.47	39±4.9*
50	12±0.6*	61±10.5*	77±3.5	99±3.35	13±5.8*
100	1±0.8*	25±1.4*	58±6.8*	91±7.12	2±1.8*
IC_{50}	27±0.5	65±5.6	>100	>100	31±3.4

3.6 Effect of CEE, Hex, DCM, EtOAc and water fractions on the pro-inflammatory cytokine production from LPS-induced RAW 264.7 macrophage cells

3.6.1 Effect of CEE, Hex, DCM, EtOAc and water fractions on the NO production of LPS-induced RAW 264.7 mouse macrophage cells

In RAW 264.7 macrophage cells, LPS stimulation can induce NO production. Therefore, this system was an excellent model for the screening of the inhibitory effect of red rice fractions on NO production *in vitro* as described in Section 2.11. Nitrite production was used as a biomarker in LPS-induced RAW 264.7 cells. The RAW macrophage cells were treated with various concentrations (0-100 µg/ml) of the red rice fractions for 2 h, and then 1 µg/ml of LPS was and furture incubated for 24 h. The Griess reagent assay was used to determine the NO production in the cell culture medium. As shown in Figure 3.38-3.42 and Table 3.28, CEE, HEX, DCM and water fractions at 100 µg/ml significantly reduced NO production by 23, 32, 18 and 16%, respectively. On other hand, EtOAc fraction had no effect on the reduced of NO production.

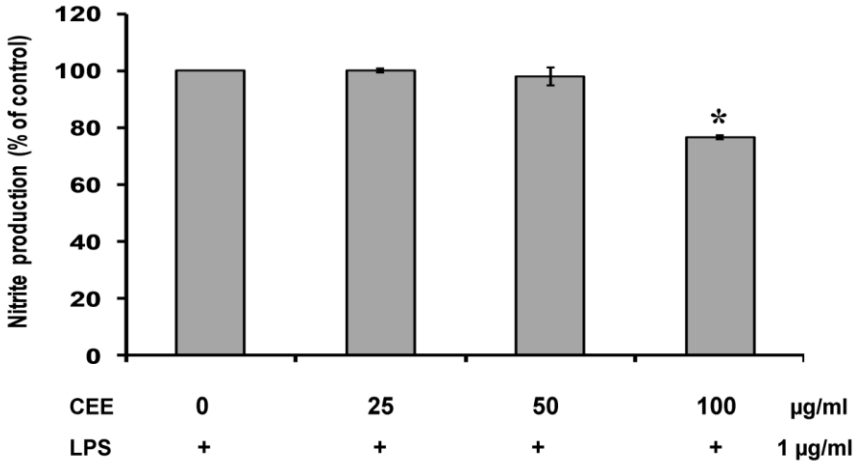

Figure 3.38 Effect of CEE fraction on the NO production in the LPS-induced RAW 264.7 cells. The cells were treated with different concentrations of CEE fraction for 2 h and then induced with LPS for 24 h. The culture supernatant was collected and analyzed for nitrite level. The data showed average values from 3 time experiments (mean ± SD). (*) $P<0.05$ was considered statistically significant vs. the LPS-treated group.

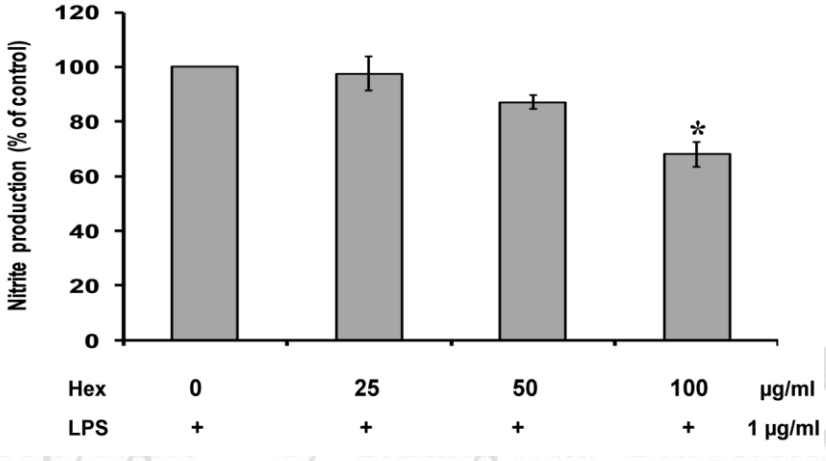

Figure 3.39 Effect of Hex fraction on the NO production in the LPS-induced RAW 264.7 cells. The cells were treated with different concentrations of Hex fraction for 2 h and then induced with LPS for 24 h. The culture supernatant was collected and analyzed for nitrite level. The data showed average values from 3 time experiments (mean ± SD). (*) $P<0.05$ was considered statistically significant vs. the LPS-treated group.

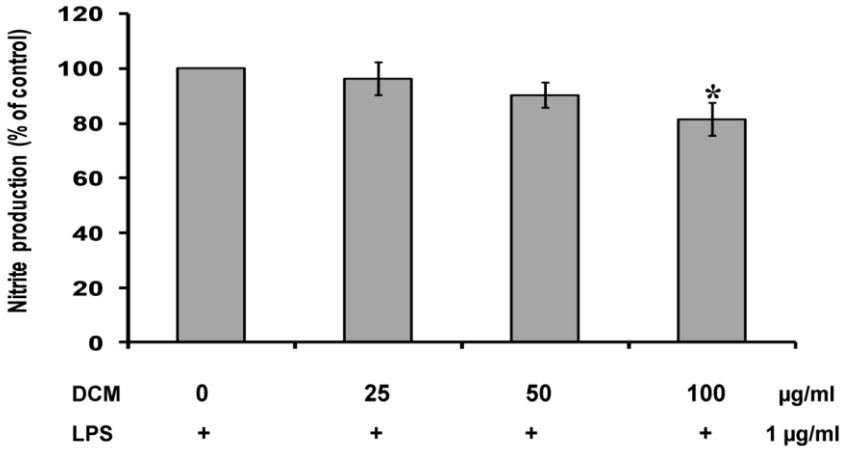

Figure 3.40 Effect of DCM fraction on the NO production in the LPS-induced RAW 264.7 cells. The cells were treated with different concentrations of DCM fraction for 2 h and then induced with LPS for 24 h. The culture supernatant was collected and analyzed for nitrite level. The data showed average values from 3 time experiments (mean ± SD). (*) $P<0.05$ was considered statistically significant vs. the LPS-treated group

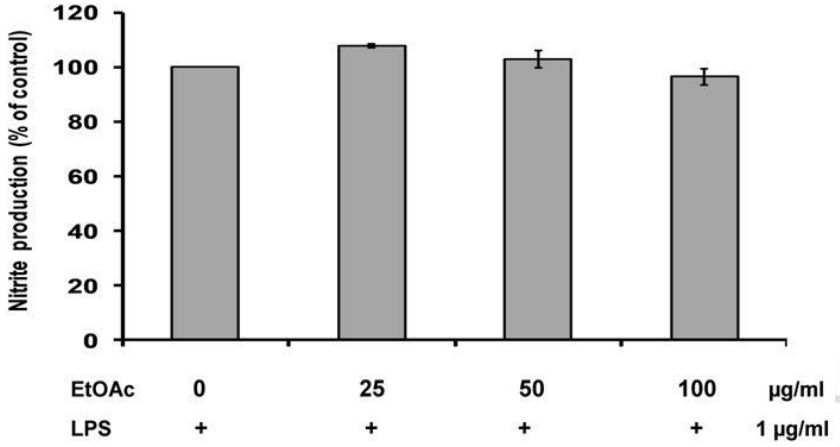

Figure 3.41 Effect of EtOAc fraction on the NO production in the LPS-induced RAW 264.7 cells. The cells were treated with different concentrations of EtOAc fraction for 2 h and then induced with LPS for 24 h. The culture supernatant was collected and analyzed for nitrite level. The data showed average values from 3 time experiments (mean ± SD). (*) $P<0.05$ was considered statistically significant vs. the LPS-treated group.

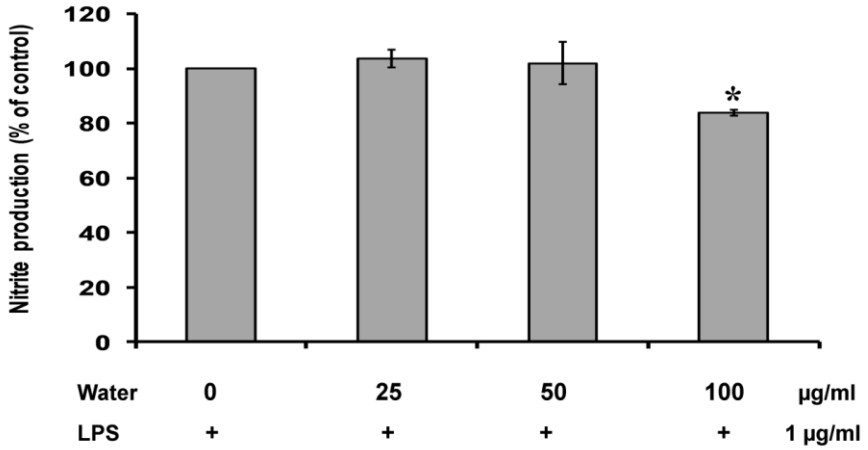

Figure 3.42 Effect of water fraction on the NO production in the LPS-induced RAW 264.7 cells. The cells were treated with different concentrations of water fraction for 2 h and then induced with LPS for 24 h. The culture supernatant was collected and analyzed for nitrite level. The data showed average values from 3 time experiments (mean ± SD). (*) $P<0.05$ was considered statistically significant vs. the group treated with LPS.

Table 3.28 Effect of CEE, Hex, DCM, EtOAc and water fractions on the NO production in LPS-induced RAW 264.7 cells. The data showed average values from 3 time experiments (mean ± SD)

Concentrations (µg/ml)	**Nitrite production (% of control)**				
	CEE	**Hex**	**DCM**	**EtOAc**	**Water**
0	100±0.0	100±0.0	100±0.0	100±0.0	100±0.0
25	100±0.7	98±6.3	96±6.0	108±0.7	104±3.2
50	98±3.2	87±2.6	90±4.6	103±3.2	102±7.8
100	77±0.8*	68±4.7*	82±6.0*	96±3.0	84±1.0*

3.6.2 Effect of CEE, Hex, DCM, EtOAc and water fractions on the production of IL-1β, IL-6 and TNF-α on LPS-induced RAW 264.7 macrophage cells

When macrophages are stimulated with LPS, they would produce various pro-inflammatory cytokines especially IL-1β, IL-6 and TNF-α. The effects of CEE, Hex, DCM, EtOAc and water fractions on LPS-induced cytokine production were thefore determined by enzyme-linked immunosorbent assay (ELISA) kits as described in Section 2.12. As shown in Figure 3.43-3.57 and Table 3.29-3.33, the production of IL-1β, IL-6 and TNF-α were significantly increased by LPS induction when compared with untreated LPS. The treatment with 100 μg/ml of CEE, HEX, DCM and water fractions significantly reduced the LPS-induced IL-1β, IL-6 production in a range of 27-34% and 21-25%, respectively, while TNF-α production was unaffected. On the other hand, EtOAc fraction had no effect on the production of IL-1β, IL-6 and TNF-α.

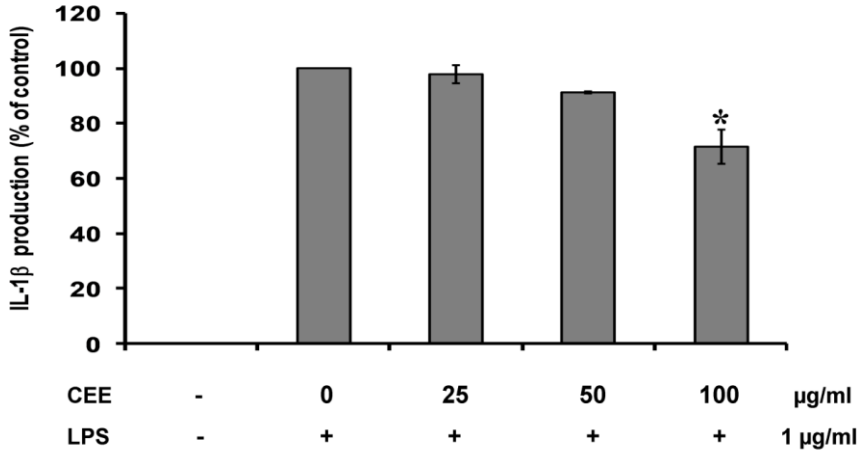

Figure 3.43 Effect of CEE fraction on IL-1β production in the LPS-induced RAW 264.7 cells. The cells were treated with different concentrations of the fraction for 2 h and induced with LPS for 24 h. The culture supernatant was collected and analyzed for IL-1β level. The data showed average values from 3 time experiments (mean ± SD). (*) $P<0.05$ was considered statistically significant vs. the LPS-treated group.

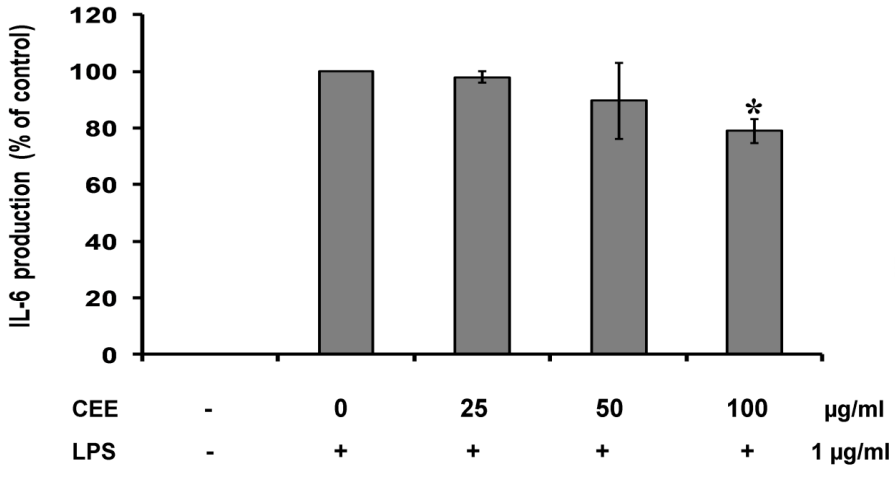

Figure 3.44 Effect of CEE fraction on the production of IL-6 in the LPS-induced RAW 264.7 cells. The cells were treated with different concentrations of the fraction for 2 h and induced with LPS for 24 h. The culture supernatant was collected and analyzed for IL-6 level. The data showed average values from 3 time experiments (mean ± SD). (*) $P<0.05$ was considered statistically significant vs. the LPS-treated group.

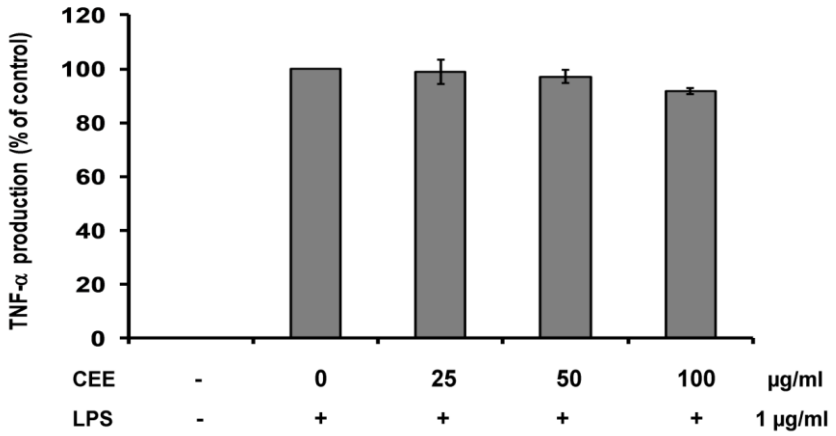

Figure 3.45 Effect of CEE fraction on the production of TNF-α in the LPS-induced RAW 264.7 cells. The cells were treated with different concentrations of the fraction for 2 h and induced with LPS for 24 h. The culture supernatant was collected and analyzed for TNF-α level. The data is represented as mean ± S.D of three independent experiments. (*) $P<0.05$ was considered statistically significant vs. the LPS-treated group.

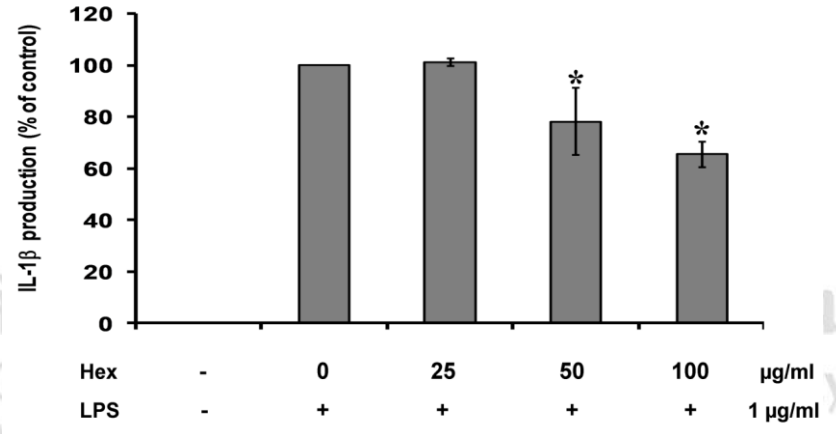

Figure 3.46 Effect of Hex fraction on the production of IL-1β in the LPS-induced RAW 264.7 cells. The cells were treated with different concentrations of the fraction for 2 h and induced with LPS for 24 h. The culture supernatant was collected and analyzed for IL-1β level. The data is represented as mean ± S.D of three independent experiments. (*) $P<0.05$ was considered statistically significant vs. the LPS-treated group

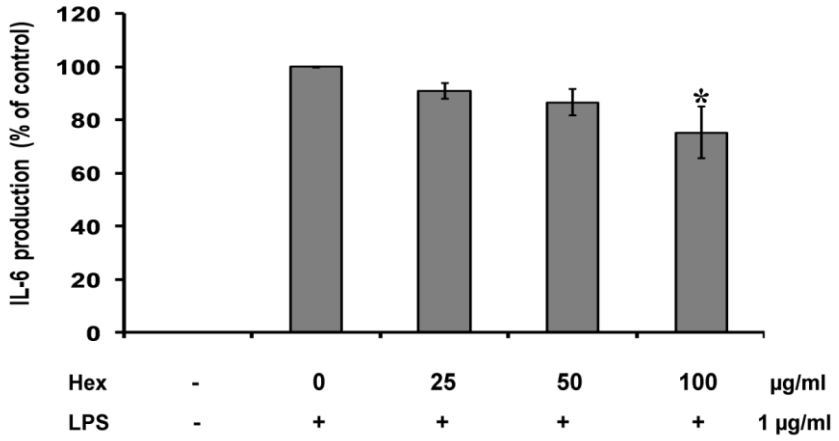

Figure 3.47 Effect of Hex fraction on the production of IL-6 in the LPS-induced RAW 264.7 cells. The cells were treated with different concentrations of the fraction for 2 h and induced with LPS for 24 h. The culture supernatant was collected and analyzed for IL-6 level. The data is represented as mean ± S.D of three independent experiments. (*) $P<0.05$ was considered statistically significant vs. the LPS-treated group.

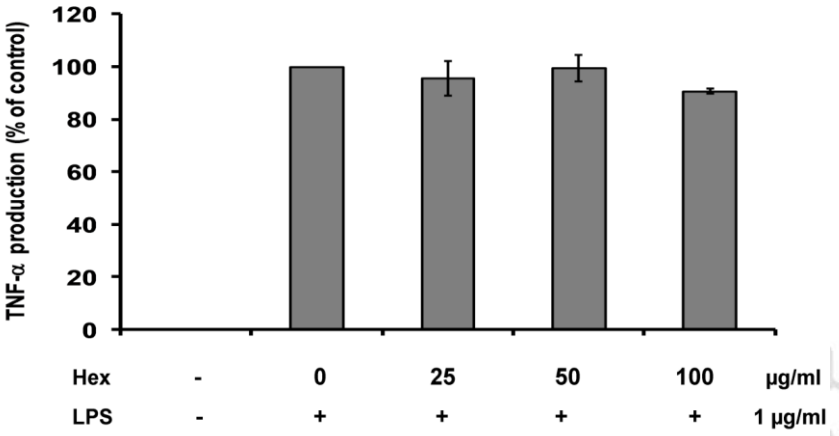

Figure 3.48. Effect of Hex fraction on the production of TNF-α in the LPS-induced RAW 264.7 cells. The cells were treated with different concentrations of the fraction for 2 h and induced with LPS for 24 h. The culture supernatant was collected and analyzed for TNF-α level. The data is represented as mean ± S.D of three independent experiments. (*) $P<0.05$ was considered statistically significant vs. the LPS-treated group.

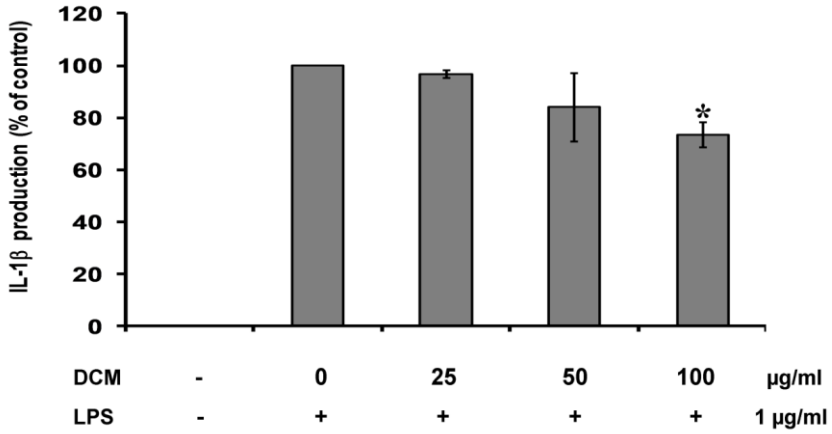

Figure 3.49. Effect of DCM fraction on the production of IL-1β in the LPS-induced RAW 264.7 cells. The cells were treated with different concentrations of the fraction for 2 h and induced with LPS for 24 h. The culture supernatant was collected and analyzed for IL-1β level. The data is represented as mean ± S.D of three independent experiments. (*) $P<0.05$ was considered statistically significant vs. the LPS-treated group.

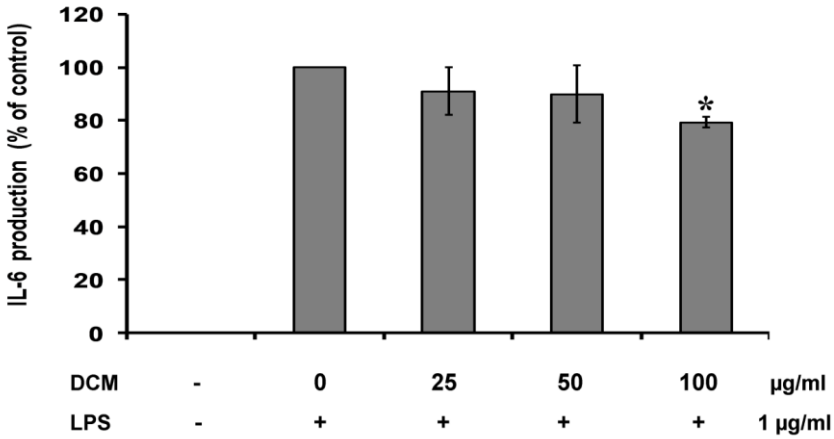

Figure 3.50 Effect of DCM fraction on the production of IL-6 in the LPS-induced RAW 264.7 cells. The cells were treated with different concentrations of the fraction for 2 h and induced with LPS for 24 h. The culture supernatant was collected and analyzed for IL-6 level. The data is represented as mean ± S.D of three independent experiments. (*) $P<0.05$ was considered statistically significant vs. the LPS-treated group.

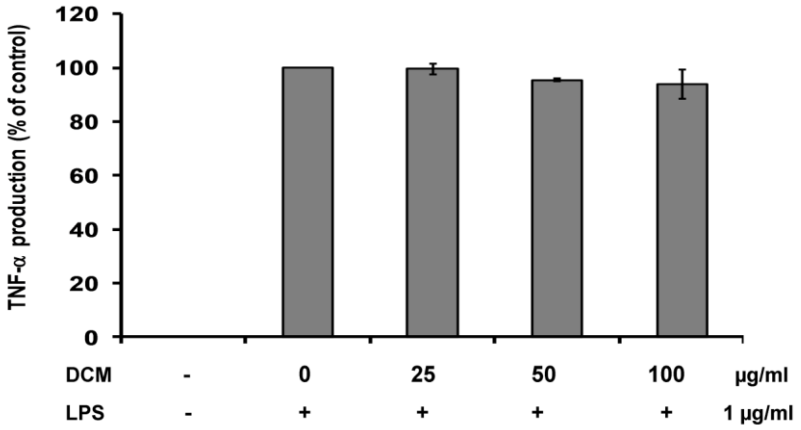

Figure 3.51 Effect of DCM fraction on the production of TNF-α in the LPS-induced RAW 264.7 cells. The cells were treated with different concentrations of the fraction for 2 h and induced with LPS for 24 h. The culture supernatant was collected and analyzed for TNF-α level. The data is represented as mean ± S.D of three independent experiments. (*) $P<0.05$ was considered statistically significant vs. the LPS-treated group.

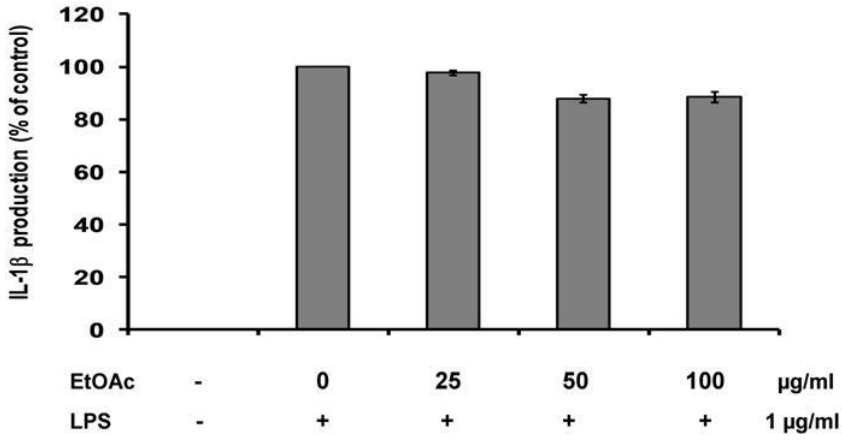

Figure 3.52 Effect of EtOAc fraction on the production of IL-1β in the LPS-induced RAW 264.7 cells. The cells were treated with different concentrations of the fraction for 2 h and induced with LPS for 24 h. The culture supernatant was collected and analyzed for IL-1β level. The data is represented as mean ± S.D of three independent experiments. (*) $P<0.05$ was considered statistically significant vs. the LPS-treated group.

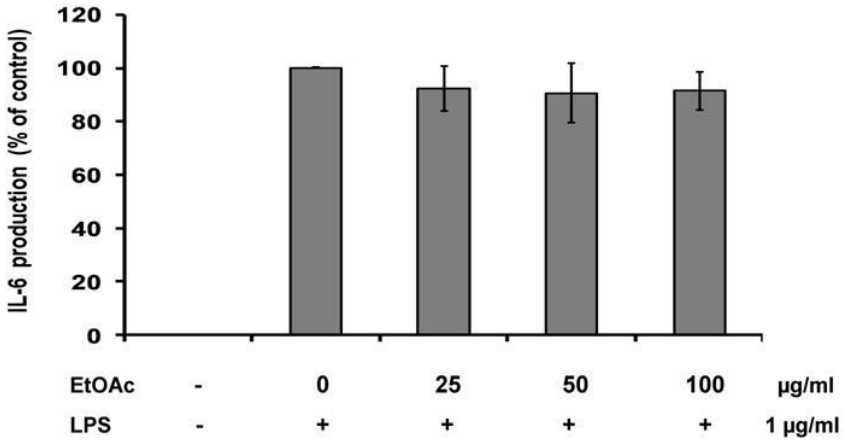

Figure 3.53 Effect of EtOAc fraction on the production of IL-6 in the LPS-induced RAW 264.7 cells. The cells were treated with different concentrations of the fraction for 2 h and induced with LPS for 24 h. The culture supernatant was collected and analyzed for IL-6 level. The data is represented as mean ± S.D of three independent experiments. (*) $P<0.05$ was considered statistically significant vs. the LPS-treated group.

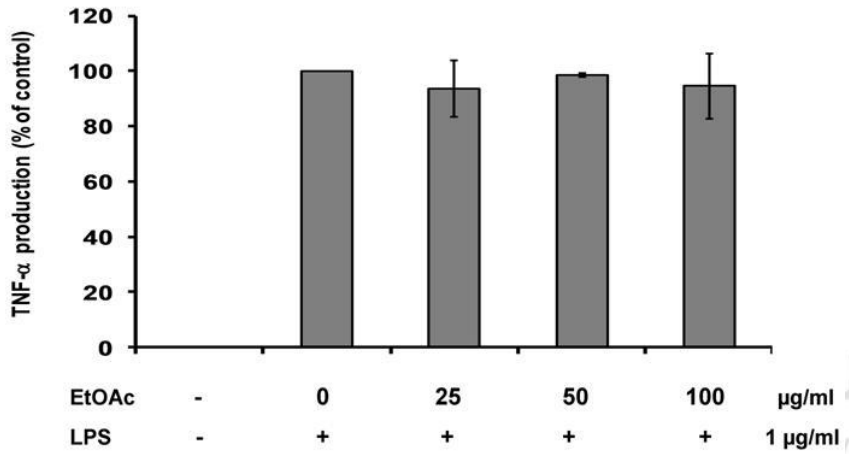

Figure 3.54 Effect of EtOAc fraction on the production of TNF-α in the LPS-induced RAW 264.7 cells. The cells were treated with different concentrations of the fraction for 2 h and induced with LPS for 24 h. The culture supernatant was collected and analyzed for TNF-α level. The data is represented as mean ± S.D of three independent experiments. (*) $P<0.05$ was considered statistically significant vs. the LPS-treated group.

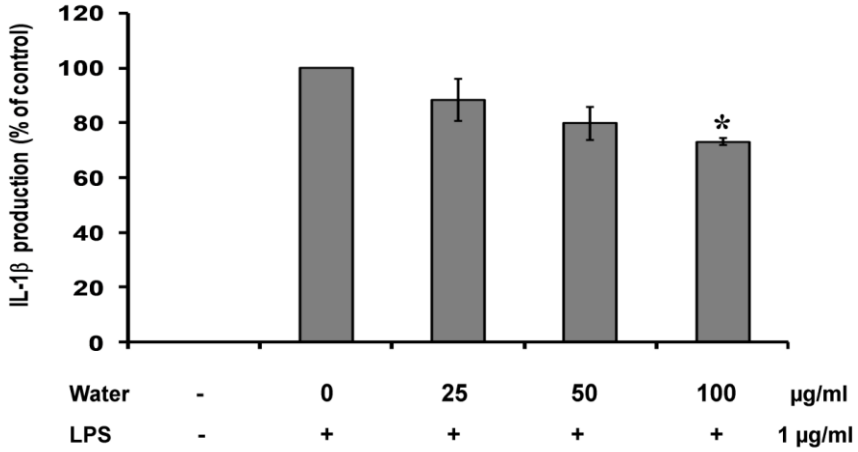

Figure 3.55 Effect of water fraction on the production of IL-1β in the LPS-induced RAW 264.7 cells. The cells were treated with different concentrations of the fraction for 2 h and induced with LPS for 24 h. The culture supernatant was collected and analyzed for IL-1β level. The data is represented as mean ± S.D of three independent experiments. (*) $P<0.05$ was considered statistically significant vs. the LPS-treated group.

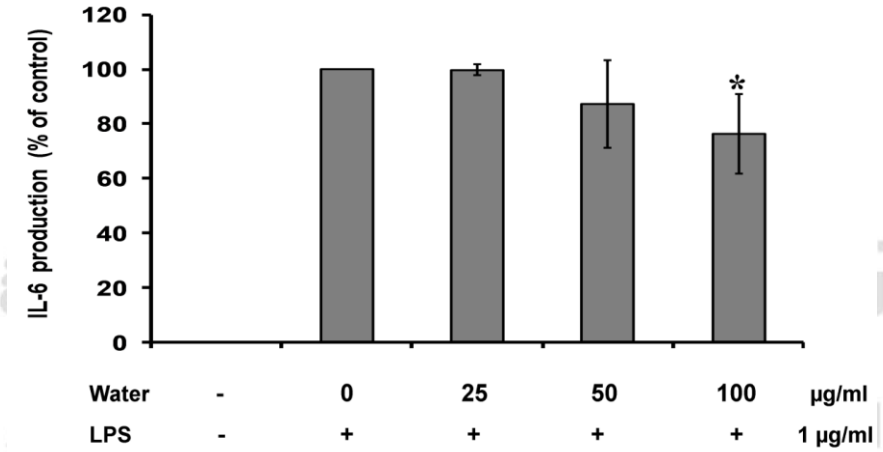

Figure 3.56 Effect of water fraction on the production of IL-6 in the LPS-induced RAW 264.7 cells. The cells were treated with different concentrations of the fraction for 2 h and induced with LPS for 24 h. The culture supernatant was collected and analyzed for IL-6 level. The data is represented as mean ± S.D of three independent experiments. (*) $P<0.05$ was considered statistically significant vs. the LPS-treated group.

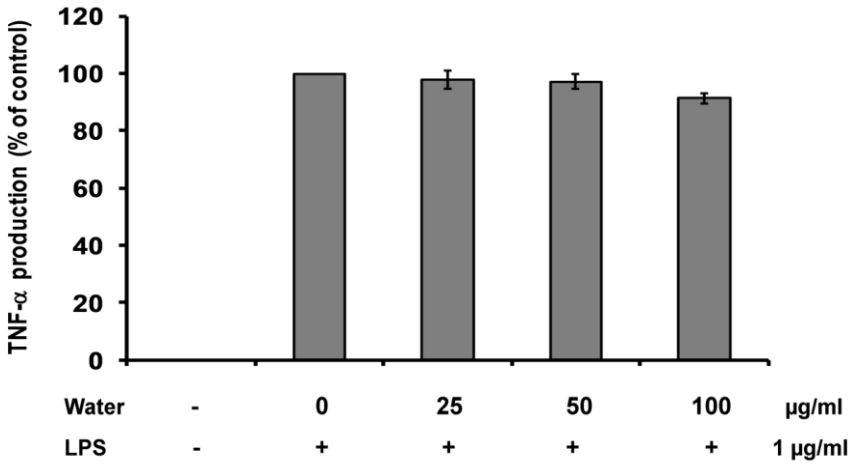

Figure 3.57 Effect of water fraction on the production of TNF-α in the LPS-induced RAW 264.7 cells. The cells were treated with different concentrations of the fraction for 2 h and induced with LPS for 24 h. The culture supernatant was collected and analyzed for TNF-α level. The data is represented as mean ± S.D of three independent experiments. (*) $P<0.05$ was considered statistically significant vs. the LPS-treated group.

Table 3.29 Effect of CEE fraction on the production of IL-1β, IL-6 and TNF-α induced by LPS in RAW 264.7 cells. The data showed average values from 3 time experiments (mean ± SD)

CEE fraction concentrations (µg/ml)	**Pro-inflammatory cytokine production (% of control)**		
	IL-1β	**IL-6**	**TNF-α**
untreated LPS	0	0	0
0	100±0.0	100±0.0	100±0.0
25	98±3.3	98±2.0	99±4.6
50	91±0.4	90±13.4	97±2.6
100	72±6.2*	79±4.1*	92±1.2

Table 3.30 Effect of Hex fraction on the production of IL-1β, IL-6 and TNF-α induced by LPS in RAW 264.7 cells. The data showed average values from 3 time experiments (mean ± SD)

Hex fraction concentrations (µg/ml)	**Pro-inflammatory cytokine production (% of control)**		
	IL-1β	**IL-6**	**TNF-α**
untreated LPS	0	0	0
0	100±0.0	100±0.0	100±0.0
25	101±1.5	91±2.8	96±6.6
50	78±13.0*	87±4.9	99±5.1
100	66±4.9*	75±9.7*	91±0.9

Table 3.31 Effect of DCM fraction on the production of IL-1β, IL-6 and TNF-α induced by LPS in RAW 264.7 cells. The data showed average values from 3 time experiments (mean ± SD)

DCM fraction concentrations (µg/ml)	**Pro-inflammatory cytokine production (% of control)**		
	IL-1β	**IL-6**	**TNF-α**
untreated LPS	0	0	0
0	100±0.0	100±0.0	100±0.0
25	97±7.6	91±9.0	100±2.0
50	84±0.6	90±10.9	95±0.6
100	73±14.3*	79±2.1*	94±5.5

Table 3.32 Effect of EtOAc fraction on on the production of IL-1β, IL-6 and TNF-α induced by LPS in RAW 264.7 cells. The data showed average values from 3 time experiments (mean ± SD)

EtOAc fraction concentrations (µg/ml)	**Pro-inflammatory cytokine production (% of control)**		
	IL-1β	**IL-6**	**TNF-α**
untreated LPS	0	0	0
0	100±0.0	100±0.0	100±0.0
25	98±1.1	92±8.4	94±10.3
50	88±1.5	91±11.1	98±0.7
100	88±2.0	91±7.2	95±11.8

Table 3.33 Effect of water fraction on the production of IL-1β, IL-6 and TNF-α induced by LPS in RAW 264.7 cells. The data showed average values from 3 time experiments (mean ± SD)

Water fraction concentrations (µg/ml)	**Pro-inflammatory cytokine production (% of control)**		
	IL-1β	**IL-6**	**TNF-α**
untreated LPS	0	0	0
0	100±0.0	100±0.0	100±0.0
25	88±7.7	100±1.9	98±3.2
50	80±6.0	87±16.0	97±2.6
100	73±1.3*	76±14.5*	91±1.9

Proanthocyanidin from red rice extract decreases invasiveness of MDA-MB-231 breast cancer cells via inhibition of the invasive proteins expression

3.7. Proanthocyanidin content determination in PRFR

3.7.1 PRFR isolation from water fraction of red rice

The water fraction of red rice extract was fractionated using a Sephadex LH-20 column chromatography. The absorbance was measured at 540 nm, to determine total proanthocyanidin contents in all fractions by vanillin assay. As shown in Figure 3.58A, the chromatographic profile of the total proanthocyanidin in the fractions that elueted by 30% methanol and 70% acetone was shown as one peak (tube No. 26-31). Fraction 28 had the highest proanthocyanidin contents compared to all fractions, and fraction 27, 29 and 30 also had fairly high content in comparison with other fractions. Therefore, fractions 27 to 29 were pooled and lyophilized, which called PRFR.

The PRFR chromatographic profiles showed the same pattern as grape seed proanthocyanidin. As shown in Figure 3.58B, the proanthocyanidin content from PRFR was co-eluted, giving similar patterns (tube No. 26-31) to the grape seed proanthocyanidin extract.

3.7.2 The content of proanthocyanidin in water fraction and PRFR

The vanillin and acid/butanol assays were used to determine the total proanthocyanidin content equivalented to standard catechin. As shown in Table 3.34, the content of proanthocyanidin in PRFR was 24.34±7.24 and 261.38±47.41 mg.g extract analyzed by vanillin and acid/butanol assays, respectively. While the content of proanthocyanidin in the water fraction was 12.45±5.32 and 95.99±2.13 mg.g extract analyzed by vanillin and acid/butanol assays, respectively.

HPLC analysis was performed after acid hydrolysis of PRFR, gallocatechin (GC), epigallocatechin (EGC), catechin (C), epicatechin (EC) were used as

standards for classification the type of proanthocyanidin (Fig 3.59A). As shown in Figure 3.59B, the peak of GC, EGC, C and EC were found in PRFR, while none of compound was detected in the non-acid hydrolysis (Fig 3.59C). The GC, EGC, C and EC are composted in the procyanidin and prodelphinidin structures. The type of proanthocyanidin included in PRFR possibly is belonging to one of these structures.

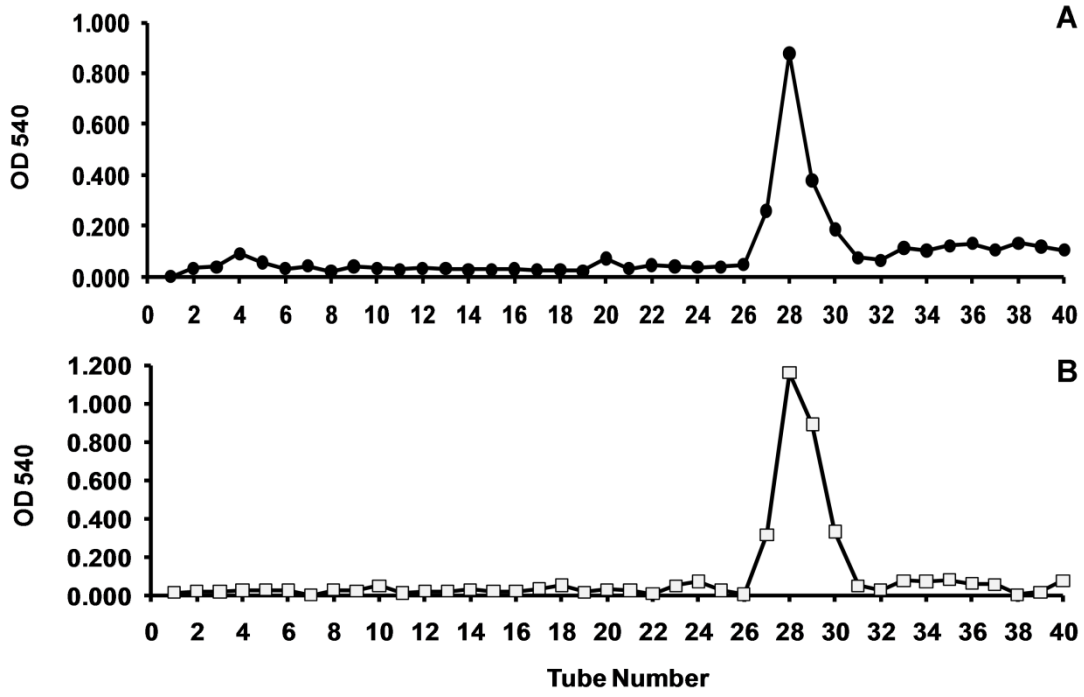

Figure 3.58. Chromatographic profiles of the PRFR fractionated by a Sephadex LH-20 column chromatography. Chromatogram A indicates the proanthocyanidin content in each fraction of the PRFR. Chromatogram B represents the proanthocyanidin content in each fraction of PRFR that co-eluated with the grape seed proanthocyanidin.

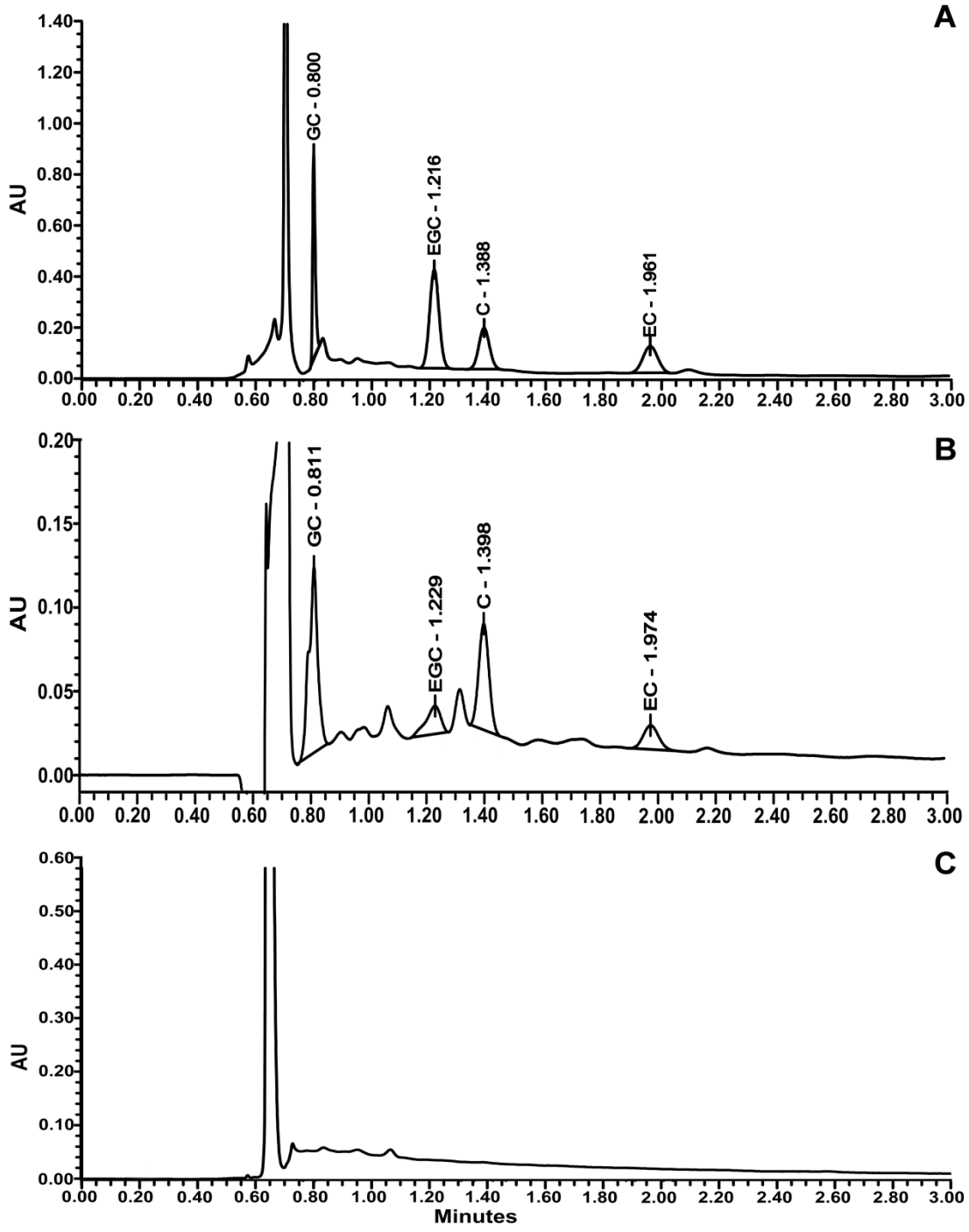

Figure 3.59. HPLC profiles of acid hydrolized PRPR (B) compared to standards (A). Chromatogram A shows HPLC profile of gallocatechin (GC), epigallocatechin (EGC), catechin (C) and epicatechin (EC) flavan-3-ol monomers stan. Chromatogram B and C shows HPLC profiles of acid hydrolyzed PRFR and non-hydrolyzed PRFR.

Table 3.34 The Total proanthocyanidins content of water fraction, PRFR and grape seed extract. The data showed average values from 3 time experiments (mean ± SD)

Fraction	**Total proanthocyanidin content (mg/g extract)**	
	Vanillin assay	**Acid/butanol assay**
Water fraction	12.43±5.32	95.99±2.13
PRFR	24.34±7.24	261.38±47.41
Grape seed extract	33.10±3.70	318.44±39.95

3.8 Cytotoxicity of PRFR on cancer cells and human skin fibroblasts

The cytotoxic effect of PRFR isolated from water fraction of red rice on the human cancer cells (MDA-MB-231, HT-1080 and SKOV-3 cells) and normal fibroblasts was analyzed by MTT assay. After treating the cells with various concentrations of PRFR (0-200 μg/ml) for 1 and 2 days, the percentage of cell survival was investigated. As shown in Figures 3.60-3.63, and Table 3.35-3.38, the cell survival was more than 80 % in the PRFR-treated cells with maximum concentration up to 200 μg/ml. The non toxic concentration of PRFR in the range 0-200 μg/ml (> 80% cell survival) was chosen for further studies.

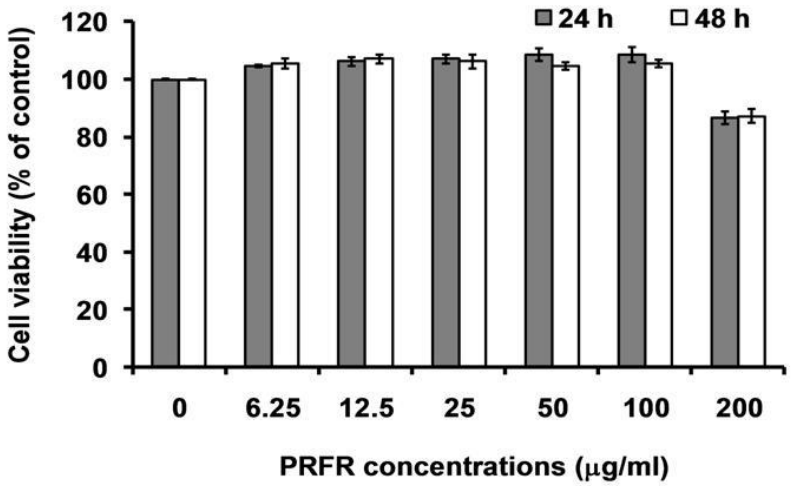

Figure 3.60 Cytotoxicity of PRFR on MDA-MB-231 cells. The cells (2.0×10^3 cell/wells) were treated with 0-200 μg/ml of PRFR for 1 and 2 days. The number of viable cells was determined by MTT assay. The results are showed as percent cell survival, compared to the control. The data showed average values from 3 time experiments (mean ± SD)

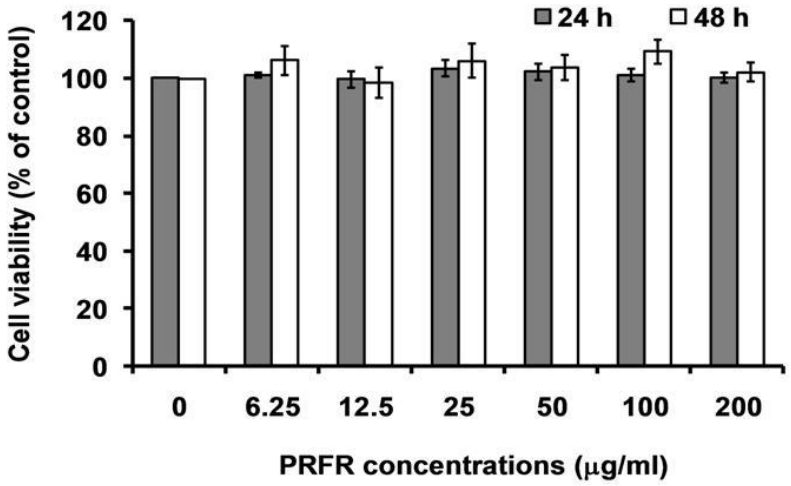

Figure 3.61 Cytotoxicity of PRFR on HT-1080 cells. The cells (2.0×10^3 cell/wells) were treated with 0-200 μg/ml of PRFR for 1 and 2 days. The number of viable cells was determined by MTT assay. The results are showed as percent cell survival, compared to the control. The data showed average values from 3 time experiments (mean ± SD)

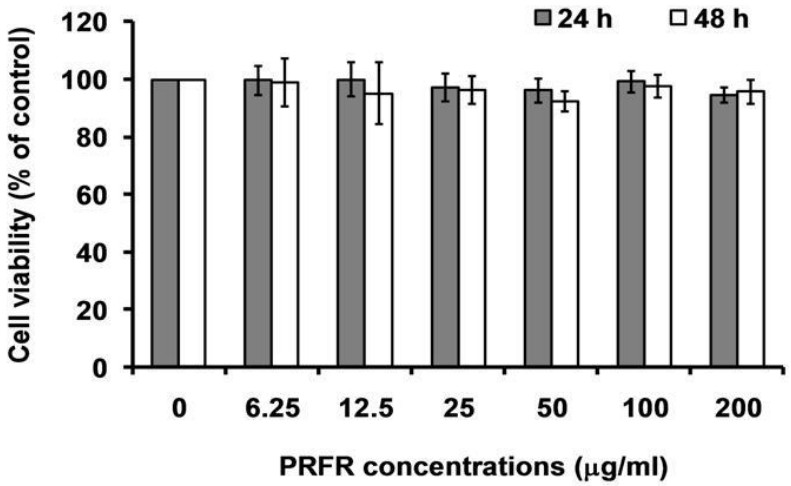

Figure 3.62 Cytotoxicity of PRFR on SKOV-3 cells. The cells (2.0×10^3 cell/wells) were treated with 0-200 μg/ml of PRFR for 1 and 2 days. The number of viable cells was determined by MTT assay. The results are showed as percent cell survival, compared to the control. The data showed average values from 3 time experiments (mean ± SD)

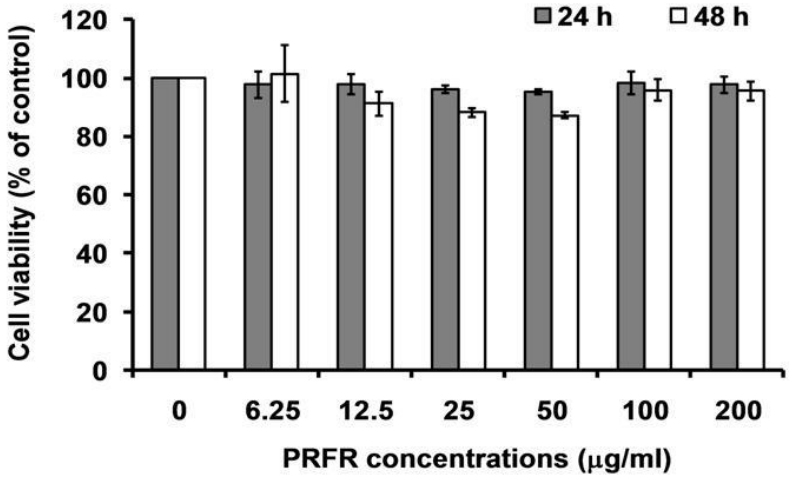

Figure 3.63 Cytotoxicity of PRFR on normal human fibroblast cells. The cells (2.0×10^3 cell/wells) were treated with 0-200 μg/ml of PRFR for 1 and 2 days. The number of viable cells was determined by MTT assay. The results are showed as percent cell survival, compared to the control. The data showed average values from 3 time experiments (mean ± SD)

Table 3.35 Cytotoxicity of PRFR on MDA-MB-231 cells for 1 and 2 days. The data showed average values from 3 time experiments (mean ± SD)

PRFR concentrations (µg/ml)	**Cell viability (% of control)**	
	1 day	**2 days**
0	100±0.0	100±0.0
6.25	105±0.60	105±1.79
12.5	106±1.55	107±1.62
25	107±1.45	106±2.47
50	109±2.23	105±1.43
100	108±2.68	106±1.31
200	87±2.09	87±2.52

Table 3.36 Cytotoxicity of PRFR on HT-1080 cells for 1 and 2 days. The data showed average values from 3 time experiments (mean ± SD)

PRFR concentrations (µg/ml)	**Cell viability (% of control)**	
	1 day	**2 days**
0	100±0.0	100±0.0
6.25	101±0.96	106±5.12
12.5	100±2.85	98±5.21
25	103±2.87	106±5.73
50	102±2.94	104±4.32
100	101±2.22	109±4.21
200	100±1.75	102±3.20

Table 3.37 Cytotoxicity of PRFR on SKOV-3 cells for 1 and 2 days. The data showed average values from 3 time experiments (mean ± SD)

PRFR concentrations (µg/ml)	Cell viability (% of control)	
	1 day	2 days
0	100±0.0	100±0.0
6.25	100±4.89	99±8.34
12.5	100±5.93	95±10.64
25	97±4.77	96±4.94
50	96±4.12	92±3.65
100	99±3.74	98±3.93
200	95±2.66	96±4.02

Table 3.38 Cytotoxicity of PRFR on normal fibroblast cells for 1 and 2 days. The data showed average values from 3 time experiments (mean ± SD)

PRFR concentrations (µg/ml)	Cell viability (% of control)	
	1 day	2 days
0	100±0.0	100±0.0
6.25	98±4.53	101±9.71
12.5	98±3.44	91±3.97
25	96±1.25	88±1.55
50	95±0.78	87±1.16
100	98±3.87	96±3.81
200	98±2.74	96±3.38

3.9 Anti-invasive effect of PRFR on MDA-MB-231 cells

To determine the anti-invasive behavior of PRFR on MDA-MB-231 cells, the modified Boyden chamber assay using the matrigel (basement membrane) coated filters was performed. As shown in Figure 3.64 and Table 3.39, treatment of the cells with PRFR for 1 day significantly reduced the number of invading cells which in a concentration dependent manner with IC_{50} at 10.22±0.45 μg/ml as compared to the control.

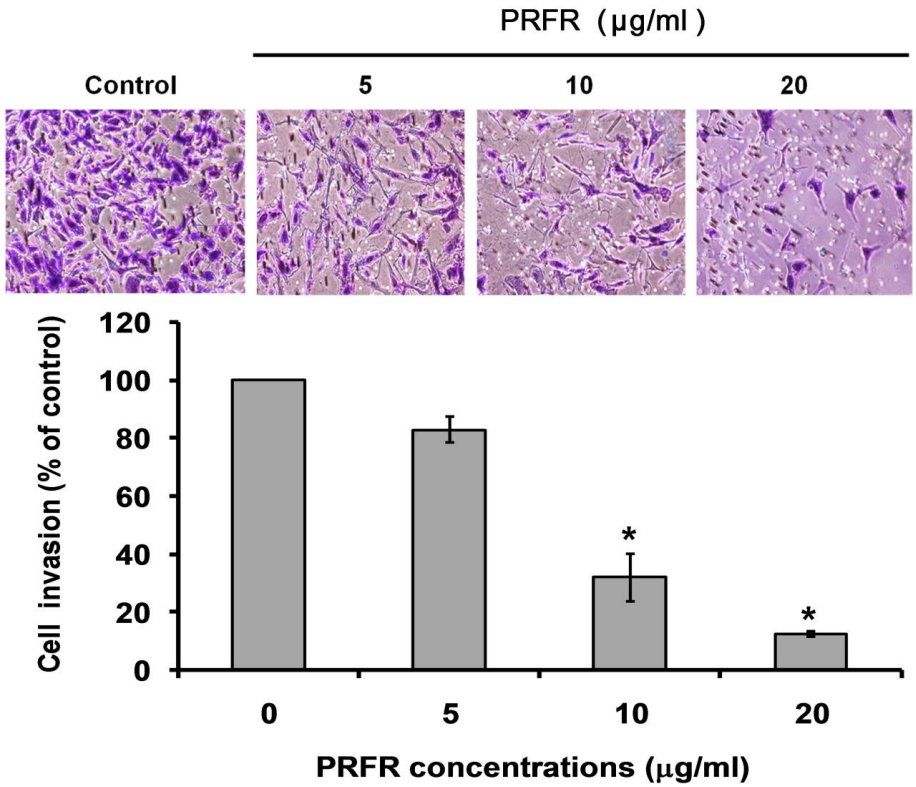

Figure 3.64 Anti-invasive effect of PRFR on MDA-MB-231 cell. The cells ($1x10^5$ cells/well) were seeded on the Matrigel-coated membrane and incubated with 0-20 µg/ml of PRFR. The cells were then allowed to invade pass through the membrane for 24 h. The invading cells were determined and the data showed average values from 3 time experiments (mean ± SD). (*) $P<0.05$ was considered statistically significant.

3.10 Anti-migration effect of PRFR on MDA-MB-231 cells

Boyden chamber migration assay was used to examine the anti-migration effect of PRFP on MDA-MB-231 cells. As shown in Figure 3.65 and Table 3.39, treatment the cells for 1 day with PRFR significantly decreased the migrated cells in a concentration dependent manner with an IC_{50} value of 10.60±0.59 μg/ml when compared to the control.

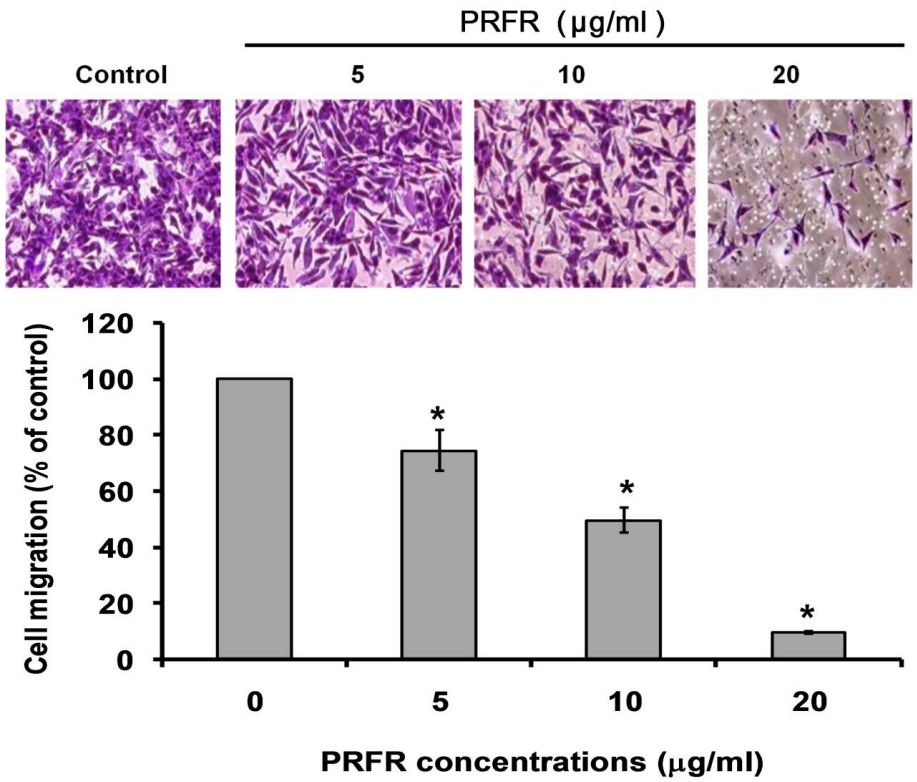

Figure 3.65 Anti-migration effect of PRFR on MDA-MB-231 cell. The cells ($1x10^5$ cells/well) were seeded on filter and incubated with 0-20 µg/ml of PRFR for 1 day. The migrated cells were analyzed and the data showed average values from 3 time experiments (mean ± SD). (*) $P<0.05$ was considered statistically significant

Table 3.39 Anti-invasion and anti-migration effect of PRFR on MDA-MB-231 cells. The data showed average values from 3 time experiments (mean ± SD)

PRFR fractions (µg/ml)	% Cell invasion	% Cell migration
0	100±0.0	100±0.0
5	83±4.49	74±7.30*
10	32±8.34*	50±4.67*
20	12±0.86*	9±0.42*
IC_{50}	10.22±0.45	10.60±0.59

3.11 Effect of PRFR on the secretion and activity of ECM degradation enzymes secreted from MDA-MB-231 cells

3.11.1 Effect of PRFR on the secretion of MMP-9

To determine whether PRFR could inhibit MMP-9 secretion from MDA-MB-231 cells, the invasive cells were treated with PRFR (0-30 μg/ml) in serum-free medium for 1 day. The MMP-9 secretion was analyzed by using gelatin zymographic assay. As shown in Figure 3.66, Table 3.40, PRFR significantly reduced the MMP-9 secretion in a concentration dependent manner with IC_{50} at 13.50±1.11 μg/ml when compared to the control.

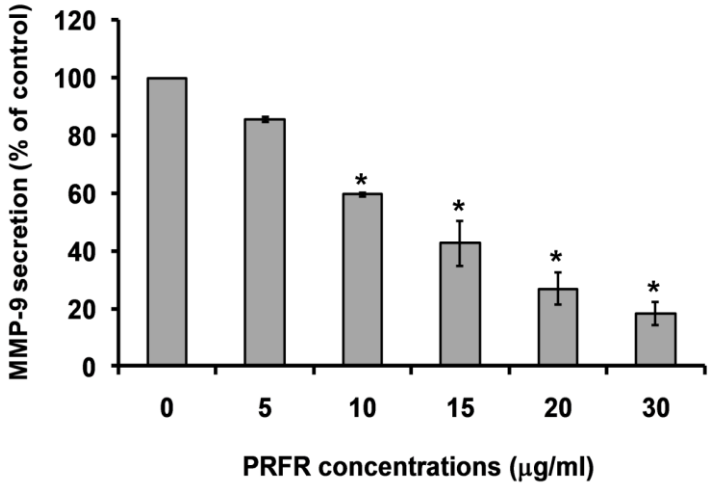

Figure 3.66 Effect of PRFR on the secretion of MMP-9 from MDA-MB-231. MDA-MB-231 cell suspension ($1x10^5$ cells/well) was incubated with 0-30 μg/ml of CEE fraction in serum free medium for 24 h. The MMP-9 gelatinolytic activities were analyzed by gelatin zymographic assay. The intensity of the gelatinolytic bands was evaluated with quantitative densitometry. the data showed average values from 3 time experiments (mean ± SD). (*) $P<0.05$ was considered statistically significant.

Table 3.40 Effect of PRFR on the secretion of MMP-9 from MDA-MB-231 cells. The data showed average values from 3 time experiments (mean ± SD)

PRFR Concentrations (μg/ml)	**MMP-9 secretion**
0	100±0.0
5	86±0.81
10	60±0.60*
15	43±7.79*
20	27±5.55*
30	18±3.91*
IC_{50}	13.50±1.11

3.11.2 Effect of PRFR on the MMP-9 activity of MDA-MB-231 cells

To determine the effect of PRFR on the MMP-9 activity in MDA-MB-231 cells, the cell culture supernatent were treated with PRFR (0-200 µg/ml) for 16 h. The activity of MMP-9 was determined by using gelatin zymographic assay. As shown in Figure 3.67 and Table 3.41, the result demonstrated that PRFR at high concentration (200 µg/ml) inhibited the activity of MMP-9 to 75±0.28% when compared to the untreated group (100%).

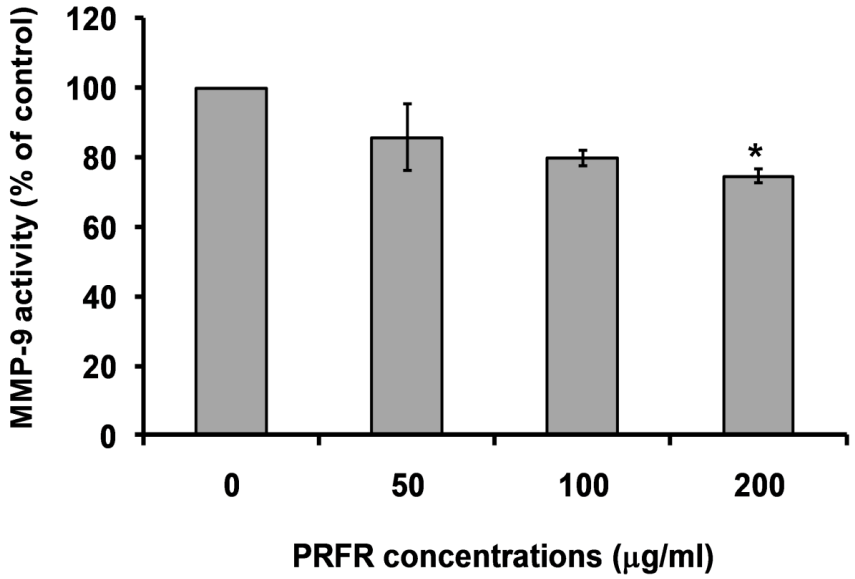

Figure 3.67 Effect of PRFR on the activity of MMP-9 secreted from MDA-MB-231 cells**.** Culture supernatant of MDA-MB-231 was collected and subjected to electrophoresis. The gelatin containing polyacrylamide gels were washed and incubated with PRFR (0-200 μg/ml) for 16 h. The intensity of the gelatinolytic bands was evaluated with quantitative densitometry .The data showed average values from 3 time experiments (mean ± SD). (*) $P<0.05$ was considered statistically significant.

Table 3.41 Effect of PRFR on the MMP-9 activity of MDA-MB-231 cells. The data showed average values from 3 time experiments (mean ± SD)

PRFR Concentrations (μg/ml)	**MMP-9 activity**
0	100±0.0
50	86±9.61
100	80±2.31
200	75±2.08*

3.11.3 Effect of PRFR on collagenase type IV activity

To investigate the inhibitory effect of PRFR on collagenase activities *in vitro* the various concentrations (0-2 μg/ml) of PRFR were incubated with collagenase type IV from *Clostridium histolyticum* and DQ gelatin substrate. The proteolytic activity of collagenase type IV was measured using fluorometric assay. Interestingly, as shown in Figure 3.68 and Table 3.42, PRFR showed a significantly inhibition of collagenase activity in a dose dependent manner with an IC_{50} at 1.46±0.04 μg/ml when compared to the control.

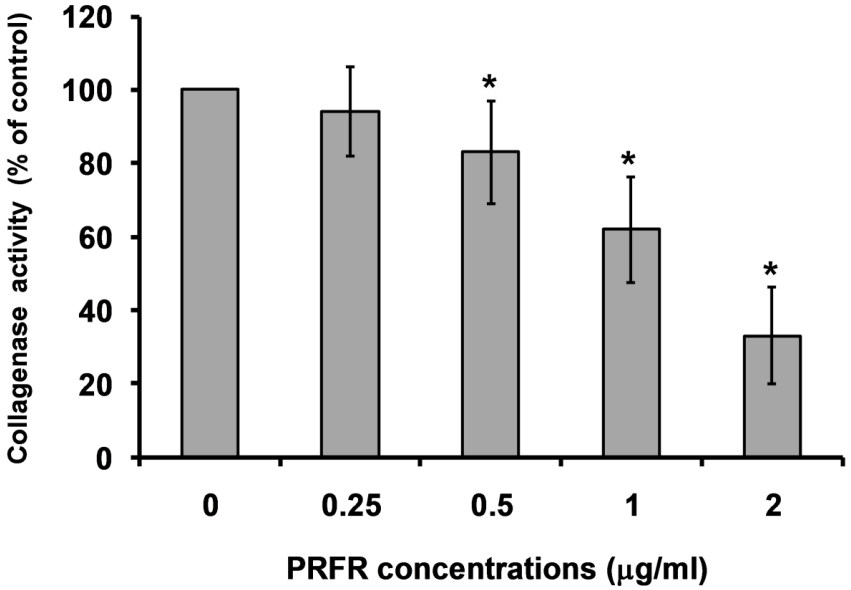

Figure 3.68 Effect of PRFR on the activity of collagenase type IV by fluorometric assay. The inhibitory effect of PRFR on proteolytic activity of collagenase was measured using gelatin fluorescence substrate. The data showed average values from 3 time experiments (mean ± SD). (*) $P<0.05$ was considered statistically significant.

Table 3.42 Effect of PRFR on the collagenase type IV activity. The data showed average values from 3 time experiments (mean ± SD)

PRFR Concentrations (μg/ml)	**MMP-9 secretion**
0	100±0.0
0.25	94±2.58
0.50	83±2.65*
1	62±5.04*
2	33±1.80*
IC_{50}	1.46±0.04

3.12 Effect of PRFR on the production of IL-6 in LPS-treated MDA-MB-231 cells

IL-6 is a pro-inflammatory cytokine that is a potential biomarker in breast cancer patients with a poor prognosis metastatic cancer. We further investigated the effects of PRFR on IL-6 production by enzyme-linked immunosorbent assay (ELISA) kits. As shown in Figure 3.69 and Table 3.43, the level of IL-6 production in culture supernatant of the cells was significantly reduced to 58±9.54% after treatment with 0-15 μg/ml of PRFR.

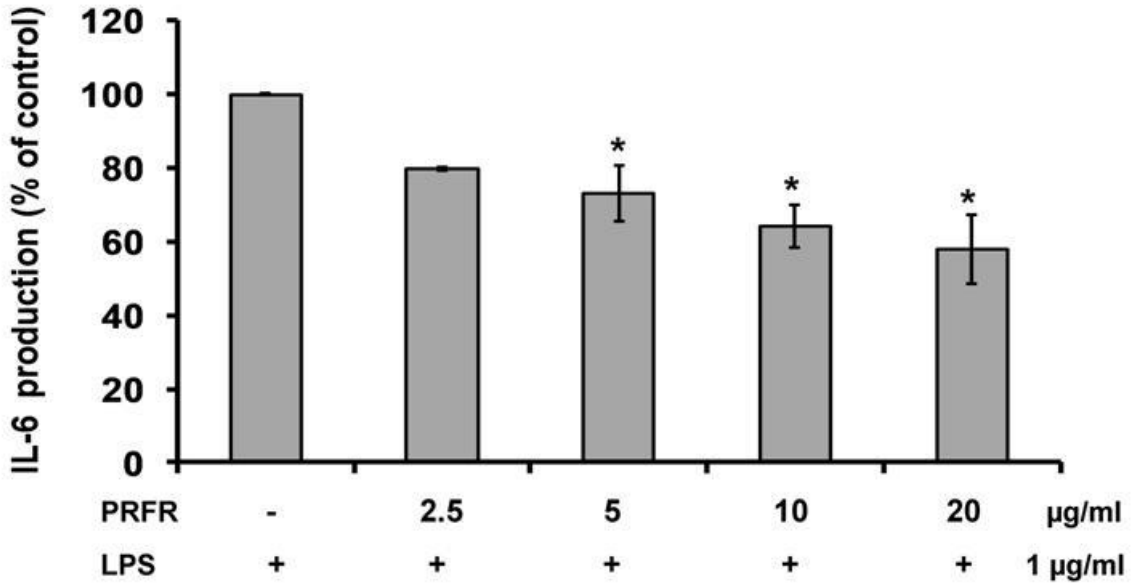

Figure 3.69 Effect of PRFR on the production of IL-6 in MDA-MB-231 cells. The cells were treated with different concentrations of PRFR for 2 h and induced with LPS for 24 h. The culture supernatants were collected and the IL-6 level was determined by ELISA. The data is represented as mean ± S.D of three independent experiments. (*) $P<0.05$ was considered statistically significant vs. the LPS-treated group.

Table 3.43 Effect of PRFR on the production of IL-6 in LPS-induced MDA-MB-231 cells. The data showed average values from 3 time experiments (mean ± SD)

PRFR concentrations (µg/ml)	**% IL-6 production**
0	100±0.0
2.5	80±0.61
5	73±7.60*
10	64±5.90*
15	58±9.54*

3.13 Inhibitory effect of PRFR on the uPA/uPAR/PAI-1 system in MDA-MB-231 cells

It has been previously reported that uPA/uPAR facilitated breast cancer metastasis. In cancer cell invasion process, there is over-expression and stimulation of MMPs and uPA system. MMP-9 and uPA are the important enzymes in breast cancer cell invasion. It was found that, PRFR could reduce secretion and activity of MMP-9 secreted from MDA-MB-231 cells. In this study, to determine the regulatory effect of PRFR on the uPA/uPAR/PAI-1 system in MDA-MB-231 cells, the cells were treated with PRFR (0-30 ug/ml) and uPA/uPAR expression and endogenous PAI-1 inhibitor were analyzed. The result from casein-plasminogen zymography assay showed that PRFR significantly reduced the secretion of uPA in a concentration dependent manner with IC_{50} value of 22.84±5.89 μg/ml (Figure 3.70 and Table 3.44). Moreover, the result from the Western blot analysis demonstrated that PRFR treatment dramatically reduced uPAR and PAI-1 expressions in a concentration dependent manner with IC_{50} values of 10.19±0.36 and 10.35±0.12 μM, respectively as shown in Figure 3.71 and Table 3.45.

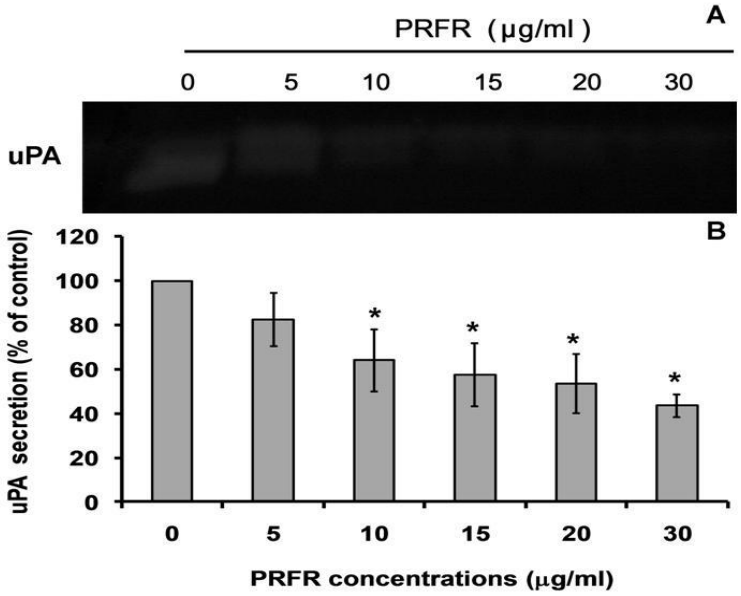

Figure 3.70 Inhibitory effect of PRFR on the uPA secretion from MDA-MB-231 cells. The cells were treated with 0-30 µg/ml PRFR for 1 day. The secretion of uPA was analyzed by casein–plasminogen zymographic assay (A). The intensity of degradating band was determined (B). The results are percentages of the control values. The data showed average values from 3 time experiments (mean ± SD); (*) $P<0.05$.

Table 3.44 Effect of PRFR on uPA secretion from MDA-MB-231 cells. The data showed average values from 3 time experiments (mean ± SD)

PRFR concentrations (µg/ml)	**% uPA secretion**
0	100±0.0
5	83±12.12
10	64±13.86*
15	58±14.43*
20	54±13.28*
30	44±5.20*
IC_{50}	22.84±5.89

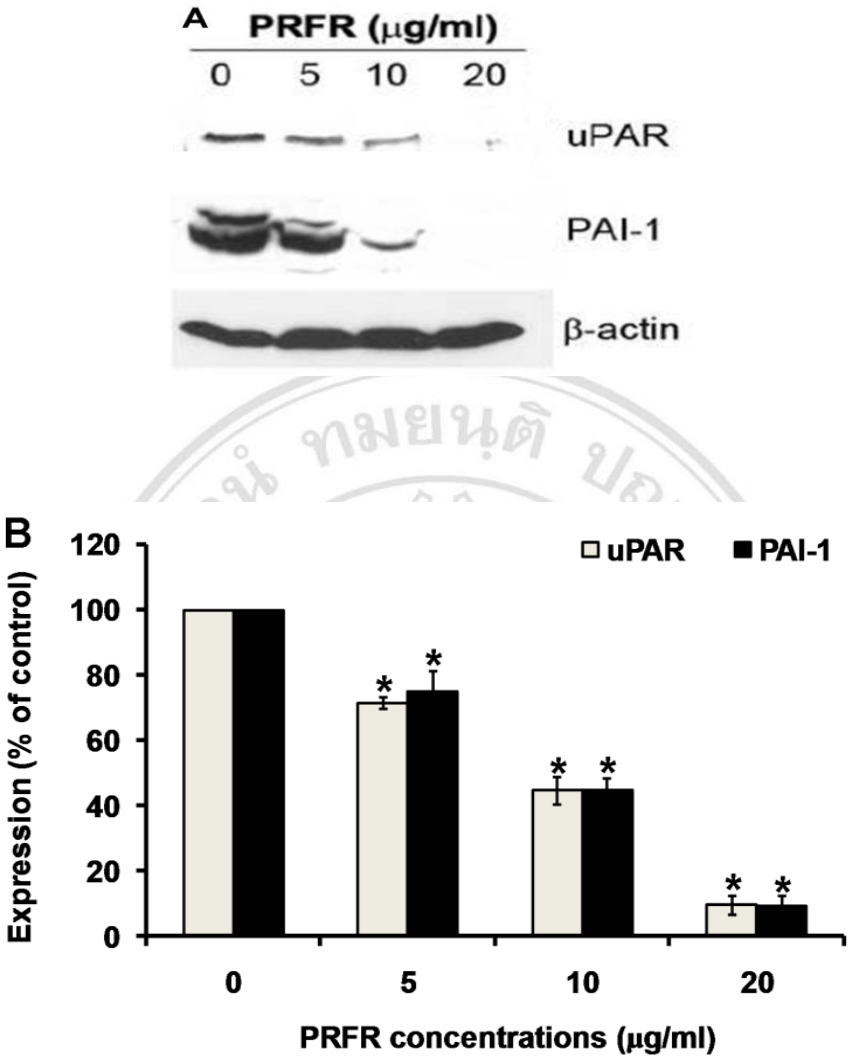

Figure 3.71 Effect of PRFR on the expression of uPAR and PAI-1 in MDA-MB-231 cells. MDA-MB-231 cells were treated with 0-20 μg/ml of PRFR for 24 h. The cells were lysated and subjected to determine uPAR and PAI-1 expression byWestern blot analysis. The intensity of the band was investigated with densitometric analysis. The data showed average values from 3 time experiments (mean ± SD). (*) $P<0.05$.

Table 3.45 Effect of PRFR on uPAR and PAI-1 expression from MDA-MB-231 cells. The data showed average values from 3 time experiments (mean ± SD)

PRFR concentrations (µg/ml)	**Protein expression (% of control)**	
	uPAR	**PAI-1**
0	100±0.0	100±0.0
5	71±1.64*	75±6.4*
10	45±4.06*	45±3.6*
20	10±2.84*	9±3.2*
IC_{50}	10.19±0.36	10.35±0.12

3.14 Inhibitory effects of PRFR on the expression of MT1-MMP in MDA-MB-231 cells

MT1-MMP is a proteolytic enzyme involved in breast cancer metastasis. Activation of MT1-MMP leads to degradation of extracellular matrix macromolecules such as fibronectin, gelatin, casein, elastin and collagens. From our previous study, PRFR could inhibit MMP-9 secretion and activity. Interestingly, it strongly inhibited collagenase activity at low concentration (< 2 μg/ml). Hence, the inhibitory effect of PRFR on MT1-MMP proteins expression levels in MDA-MB-231 cell was assessed by Western blot method as described in Section 2.24. As shown in Figure 3.72, Table 3.46, PRFR significantly reduced the protein expression of MT1-MMP in a concentration dependent manner with IC_{50} value of 10.44±0.64 μg/ml.

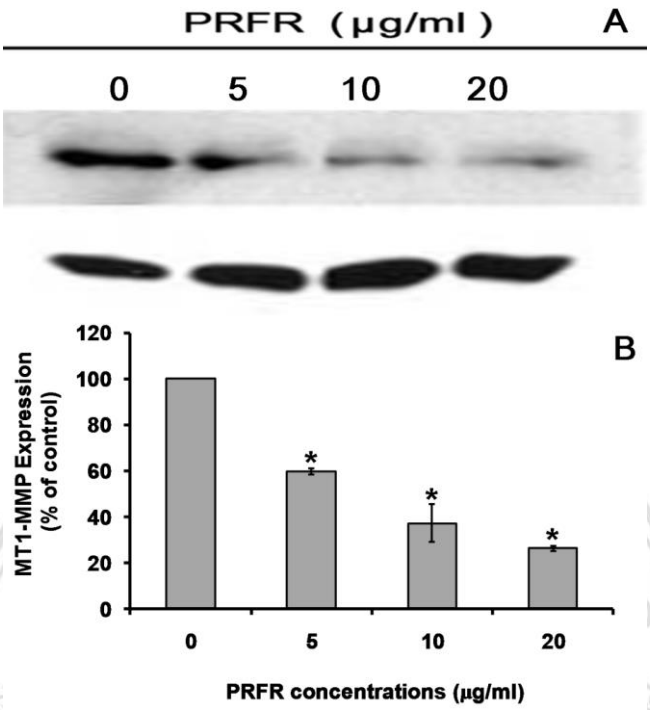

Figure 3.72 Inhibitory effect of PRFR on the expression of MT1-MMP in MDA-MB-231 cells. The cells were treated with 0-20 µg/ml of PRFR for 1 day. The expression of MT1-MMP was assessed by Western blotting. The intensity of the band was quantified by densitometry, where control group represent 100%. The data showed average values from 3 time experiments (mean ± SD). (*) $P<0.05$.

Table 3.46 Effect of PRFR on the expression of MT1-MMP in MDA-MB-231 cells. The data showed average values from 3 time experiments (mean ± SD)

PRFR concentrations (µg/ml)	**% MT1-MMP expression**
0	100±0.0
5	60±1.39*
10	37±8.15*
20	26±1.19*
IC_{50}	10.44±0.64

3.15 Inhibitory effects of PRFR on the expression of ICAM-1, an adhesion molecule

In human breast cancer cell, ICAM-1 is strongly expressed and plays a significant role in invasion, migration and metastasis. Moreover, the up-regulation of this adhesion molecule is found in response to various cytokines and is associated with inflammatory responses. Interestingly, from our previous study, PRFR could inhibit the invasion, migration and IL-6 inflammatory cytokine production in MDA-MB-231 cell. Therefore, the inhibitory effect of PRFR on ICAM-1 proteins expression in MDA-MB-231 cell was analyzed by Western blotting as described in Section 2.24. As shown in Figure 3.73, Table 3.47, PRFR significantly recued the protein level of ICAM-1 in a concentration dependent manner with IC_{50} value of 15.95±0.88 µg/ml.

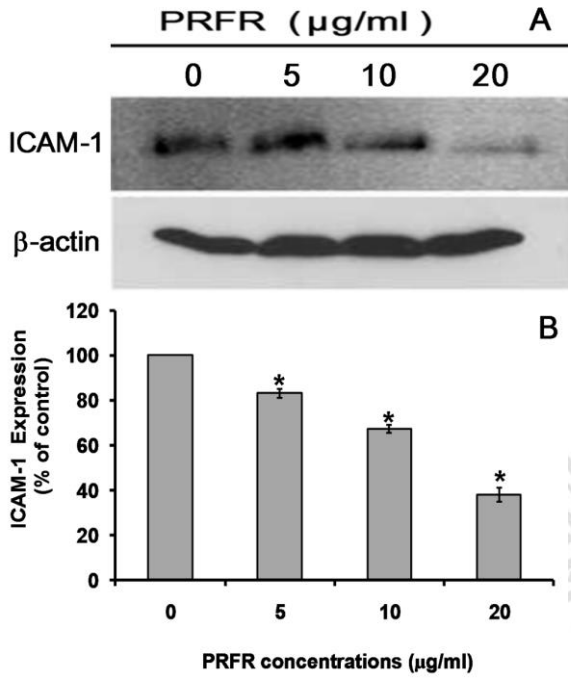

Figure 3.73 Inhibitory effect of PRFR on the expression of ICAM-1 in MDA-MB-231 cells. The cells were treated with 0-20 µg/ml of PRFR for 1 day. The expression of ICAM-1 was determined by Western blot analysis. The intensity of the band was quantified by densitometry, where control group represent 100%. The data showed average values from 3 time experiments (mean ± SD). (*) $P<0.05$.

Table 3.47 Effect of PRFR on the expression of ICAM-1 in MDA-MB-231 cells. The data showed average values from 3 time experiments (mean ± SD)

PRFR concentrations (µg/ml)	**% ICAM-1 expression**
0	100±0.00
5	83±1.93*
10	67±1.73*
20	38±3.19*
IC_{50}	15.95±0.88

3.16 Effect of PRFR on the NF-κB DNA binding activity

NF-κB regulates cancer cell metastasis by enhancing the expression of MMPs, uPA, uPAR, cytokine and ICAM-1. The inhibitory effect of PRFR on the activity of NF-κB binding to DNA was investigated as described in Section 2.25. As shown in Figure 3.74 and Table 3.48, DNA binding activity of NF-κB was significantly inhibited when the cells were treated with PRFR in a concentration dependent manner with IC_{50} at 9.17±1.17 μg/ml.

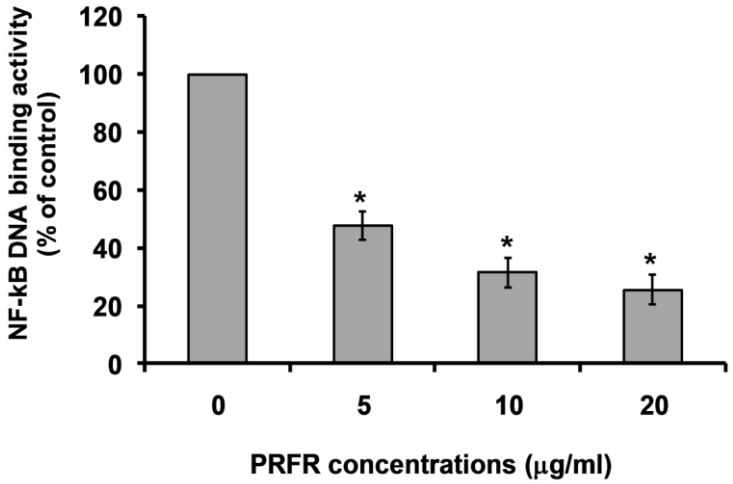

Figure 3.74 Effect of PRFR on NF-κB DNA binding activity in MDA-MB-231 cells. The cells were incubated with (0-20 μg/ml) of FRFR for 1 day, and then nuclear extracts were prepared. NF-κB binding activity was determined by using ELISA assay. The data showed average values from 3 time experiments (mean ± SD). (*) $P<0.05$

Table 3.48 Effect of PRFR on NF-κB DNA binding activity in MDA-MB-231 cells. The data showed average values from 3 time experiments (mean ± SD)

PRFR concentrations (μg/ml)	**NF-κB DNA binding activity (%of control)**
0	100±0.0
5	48±4.97*
10	32±5.13*
20	26±5.17*
IC50	9.17±1.17